# 3

# POLARIZABILITY MODELING OF HETEROGENEOUS MEDIA

*A. H. Sihvola and I. V. Lindell*

## 3.1 Introduction

Mixing rules relating the macroscopic dielectric properties of heterogeneous media to those of their constituent phases and the internal structure of the mixture have been a subject of electrical research for a long time: the earliest mixing formulas originate from the end of the nineteenth century. The ability of treating a random medium with effective parameters that contain information how the inhomogeneities of the material affect the electric field behavior is essential to researchers in the fields of, for example, remote sensing, industrial and medical applications of microwaves, and materials science.

In low-frequency modeling of composite materials, the concept of effective permittivity is practically indispensable. This quantity, the effective permittivity or macroscopic dielectric constant can be used to describe media that are homogeneous to the extent that no scattering effects are significant as radio waves penetrate these materials. If there are inhomogeneities in the material – and there always are if the microscopic level is considered deeply enough – these should be considerably smaller in size than the spatial variation of the incident electromagnetic field, i.e. its wavelength. In this low-frequency region the scattering effects from the inclusions are avoided. In radio wave propagation problems and remote sensing applications, the normal situation is that geophysical media encountered are composed of materials with dielectrically different properties, and effective permittivity is a quantity of much use: it is measured and it is connected with the constituent properties by empirical formulae. This is the case for many natural media like snow, lake ice, sea ice, soil, vegetation, and hydrometeors: rain, hail, or even dust storms.

A theoretical approach to the problem of the effective permittivity of dielectric mixtures calls for calculation of the polarizabilities and dipole moments of the scatterers, or inclusions, that compose the mixture. The dipole moments of simple discrete inclusions like spheres or ellipsoids are known and the mixing formula for a two-phase mixture with spherical inclusions can be presented in a simple symmetrical form. To solve the polarizability of a general inclusion, two methods are possible: the internal field and the external field approach. The internal field approach solves the dipole moment by integrating the product of the field and the permittivity over the inclusion volume whereas the external field approach studies the field perturbation due to the inclusion, which gives the amplitude of an equivalent dipole.

This presentation mainly focuses on the polarizability properties of inclusions with well-defined bulk permittivities. Less attention is paid on the primary physical mechanisms responsible for the polarization. According to the Clausius-Mossotti formula, polarizabilities due to different polarization mechanisms are additive, but, on the molecular level, this has been questioned by the Onsager theories for the case of mixtures with polar molecules, which contain permanent dipole moments. This discrepancy will be discussed shortly in a section but outside it, it is assumed that the different polarization components are additive.

Attention is also focused on mixtures where the inclusions need not be seen as discrete scatterers but rather the whole mixture as a continuous random medium. A concise review is given about our work on this topic: the calculation of the polarizabilities and dipole moments of scatterers of different shape and structure and the effective permittivity of mixtures composed of these scatterers. The restriction still holds that the spatial correlation distance of the material be smaller than the wavelength. This requirement being met, the magnitude of the permittivity contrast (permittivity ratio between the inclusion and the background) is not restricted by the non-scattering limitation.

Formulae for mixtures with homogeneous spheres and ellipsoids have been presented in [1]. Also the case of mixtures with inclusions of a spherical core and a spherical shell has been solved [2]. The polarizability of multilayer spheres is studied in [3] by a transmission line analogy. More generally, the effective permittivity of mixtures with inclusions that possess continuous radial permittivity profile has been treated in [4]. The effective permittivity will depend on the permittivities of the constituent materials, their volume fractions, and naturally on the functional form of the permittivity profile. Also, analysis of mixtures where the scatterers are layered or continuously inhomogeneous ellipsoids [5] leads to ellipsoidal coordinates but the results from the spherical geometries are generalizable, provided that the inhomogeneity (partial or continuous) can be expressed as a function of only one ellipsoidal coordinate.

For some problems, a variational method is the most suitable way for finding out the polarizability and the dipole moment [4]. A stationary functional is derived which can be used to obtain accurate estimates for the polarizability even if the field variation due to the inclusion is not known. This is because the nature of stationary functionals is such

that by knowing only approximately the variation of the fields, the scalar polarizability resulting from the functional is much more accurate than the field values that are not of interest. The mixtures with Gaussian packets – a truly continuous random medium the permittivity function of which is everywhere differentiable – are solved by the variational approach.

Only for sparse mixtures is the mixing formula unique. For dense mixtures, mixing rules are not unambiguous: the multitude of mixing formulas presented in the literature is a reflection of the randomness in the structure of these heterogeneous materials of interest. There is no exact solution for the electromagnetic problem with random parameters and boundaries producing formidably many degrees of freedom, and therefore rivaling mixing theories that receive experimental confirmation can coexist. Common to all of the mixing theories is the basic requirement for the validity of their use: the spatial variation of the electric field has to be less than the variation in the structure of the medium. In this paper, a way to describe these different aspects of self-consistency is attempted by introducing a concept of "apparent permittivity" [1], [6].

Although scattering losses cannot be included in the effective permittivity due to the quasistatic restriction, absorption losses are taken care of. If the component permittivities are lossy, also the mixture permittivity is: it is a complex number. Numerical illustrations about the propagation attenuation of microwaves due to melting hail exploit this property. In the application section, also dry snow is modeled.

The effective permittivity is a low-frequency concept, and the question can be raised, what is the frequency limit of its applicability. To answer this, formulas are presented that take into account the first scattering term that has effect at lower frequencies. The third power of frequency appears in these formulas in connection with the radius of the scatterers, and comparing the absorption and scattering contributions to the imaginary part of the effective permittivity, upper-limit frequency can be determined for the range where scattering phenomena can be neglected, given the desired accuracy for the permittivity.

## 3.2 Effective Permittivity

In this section, the effective permittivity of a mixture will be defined and its connection to the polarization and dipole moments of the

scatterers composing the heterogeneous medium is derived. The relation connecting the effective permittivity and polarizabilities depends on the shape of the inclusions and is given for spheres and ellipsoids. However, this relation is independent of the internal structure of the scatterer.

### *a. The effective Permittivity and the Exciting Field*

Consider a mixture with dielectric background material of permittivity $\epsilon_0$ containing $n$ inclusions in unit volume, each of polarizability $\alpha$. The background permittivity $\epsilon_0$ need not be that of free space; it can have any value, even complex: in mixing formulae that result from the analysis, only the relative permittivities of the component permittivities with respect to $\epsilon_0$ have effect. Inclusion permittivities can also be smaller than the background dielectric constant as is the case for calculating the effective permittivity of sea ice, for example. There, $\epsilon_0$ can be considered as the permittivity of pure ice, and among the scatterers there are air bubbles with smaller dielectric constant. This notation for $\epsilon_0$ is therefore a deviation from the classical absolute definition, where the permittivity is referred to vacuum.

The effective permittivity or the macroscopic permittivity $\epsilon_{\text{eff}}$ is defined as the ratio between the average displacement $\overline{D}$ and the average field $\overline{E}$:

$$\overline{D} = \epsilon_{\text{eff}} \overline{E} \tag{1}$$

The displacement depends on the average polarization $\overline{P}$ in the material

$$\overline{D} = \epsilon_0 \overline{E} + \overline{P} \tag{2}$$

The average polarization can be calculated from the dipole moments $\overline{p}$ of the inclusions; it is the dipole moment density in this polarizable material

$$\overline{P} = n\overline{p} \tag{3}$$

The dipole moment of an inclusion depends on its polarizability and the exciting field $\overline{E}^e$

$$\overline{p} = \alpha \overline{E}^e \tag{4}$$

Here, the exciting field is the same as the average field only for very sparse mixtures where there is little polarization, or the inclusions are far from each other and do not contribute an extra field term to the adjacent inclusions. For problems where this is not the case, the permeating polarization due to surrounding inclusions has to be taken into

account. The manner and magnitude how this affects the exciting field depends on the shape of the inclusion. The exciting field is the sum of the macroscopic field $\overline{E}$ and the depolarization field that can be calculated from the decomposition given by Yaghjian [7–8]

$$\overline{E}^e = \overline{E} + \frac{1}{\epsilon_0}\overline{\overline{L}} \cdot \overline{P} \tag{5}$$

Here, the source dyadic $\overline{\overline{L}}$ depends on the shape of the inclusion volume and in [7] and [8], the integral representation is given to enumerating it for any shape.

### *b. Spherical Inclusions*

For spherical shape, the source dyadic is $\overline{\overline{L}} = \overline{\overline{I}}/3$, where $\overline{\overline{I}}$ is the unit dyadic. Hence, the exciting field is

$$\overline{E}^e = \overline{E} + \frac{\overline{P}}{3\epsilon_0} \tag{6}$$

Yaghjian derived the field decomposition for the calculation of fields in the source region, giving the restriction of the inclusion size for numerical calculation: the maximum chord length $d_{\max}$ of a single inclusion is limited by $d_{\max} \simeq \lambda/2\pi$ where $\lambda$ is the wavelength of the incident field. This requirement imposes also the quasistatic restriction for the size of the inclusions in the mixture when the concept of effective permittivity is used: they should be smaller than about a sixth of a wavelength. If the background medium of the mixture is not air but an optically denser material, also the quasistatic restriction becomes more severe: the maximum chord length is still smaller by a factor of square root of the permittivity of the background medium $\epsilon_0$.

From the equations above, the effective permittivity can be calculated as a function of the dipole moment density $n\alpha$:

$$\epsilon_{eff} = \epsilon_0 + 3\epsilon_0 \frac{n\alpha}{3\epsilon_0 - n\alpha} \tag{7}$$

This equality can also be written in the form of the Lorentz-Lorenz formula (also known as the Clausius-Mossotti formula) [9]

$$\frac{\epsilon_{\text{eff}} - \epsilon_0}{\epsilon_{\text{eff}} + 2\epsilon_0} = \frac{n\alpha}{3\epsilon_0} \tag{8}$$

The problem is how to calculate the dipole moment induced in the inclusions, which gives the polarizability $\alpha$. This entails solving the internal field of an inclusion in a quasistatic field, i.e. finding the solution of the Laplace equation.

It is worth noting that the inclusions in the mixture need not be of the same size. As long as each of the inclusions satisfies the quasistatic requirement, their polarizabilities are the same and have to be multiplied with the volume fraction to sum up to the average polarization, (8) being perfectly valid. On the other hand, if the mixture contains inclusions with different polarizabilities, like, in the simplest case, for example spheres of $N$ different permittivities, they have to be multiplied by their individual volume fractions $n_i$, and (8) has to be modified into:

$$\frac{\epsilon_{\text{eff}} - \epsilon_0}{\epsilon_{\text{eff}} + 2\epsilon_0} = \sum_{i=1}^{N} \frac{n_i \alpha_i}{3\epsilon_0} \tag{9}$$

The use of this formula requires that the different types of inclusions be distributed homogeneously in the mixture when regarding scales of the order of wavelength. The sum in this formula is replaced by an integral for the case of continuous permittivity distribution of inclusions.

### *c. Clausius-Mossotti Formula Versus Onsager Formula*

In the analysis above, (8), the polarizability $\alpha$ is the sum of all polarization mechanisms: electronic, atomic, ionic, and interfacial polarizations (for discussion on different polarization types, see [10]). On the molecular level, there has been discussion on the validity of this additiviness of polarizabilities in the case of mixtures that contain polar molecules, like water. The Clausius-Mossotti formula has been challenged by the Onsager formula, which is derived by considering separately two components of the exciting field: the cavity field (i.e. the Lorentz field) and the reaction field. This reaction field acts upon the dipole as a result of electric displacements induced by its own presence [11].

In the Clausius-Mossotti formula, the orientation polarization $\alpha_{\text{or}}$ due to polar dipoles is one component of the total polarizability $\alpha$:

$$\alpha_{\text{or}} = \frac{\mu^2}{3k_B T} \tag{10}$$

where $\mu$ is the permanent dipole moment of the molecule, $k_B$ is Boltzmann's constant, and $T$ is temperature. The Onsager formula reads:

$$\frac{(\epsilon_{\text{eff}} - \epsilon_{\text{np}})(2\epsilon_{\text{eff}} + \epsilon_{\text{np}})}{\epsilon_{\text{eff}}(\epsilon_{\text{np}} + 2\epsilon_0)^2} = \frac{n\mu^2}{9\epsilon_0 k_B T} \tag{11}$$

Here, $\epsilon_{\text{np}}$ is the effective permittivity with no polar molecules in the mixture, and the Onsager formula gives the correction to this value due to the permanent dipoles. It can be seen that with no polar molecules present, the Clausius-Mossotti formula and the Onsager formula are equal. With the Onsager formula, ferroelectric properties of materials have been explained, for which the temperature plays a central role.

Further analysis on the role of polar molecules in suspensions have been performed by Kirkwood and Fröhlich (see, for example [12]).

### *d. Ellipsoidal Inclusions*

For ellipsoidal inclusions, the depolarization dyadic is diagonal

$$\overline{\overline{L}} = \sum_{i=1}^{3} N_i \hat{u}_i \hat{u}_i \tag{12}$$

where $\hat{u}_i$ are unit vectors in the three orthogonal axial directions of the ellipsoid and $N_i$ are the corresponding depolarization factors of the ellipsoid:

$$N_a = \frac{abc}{2} \int_0^\infty \frac{ds}{(s + a^2)\sqrt{(s + a^2)(s + b^2)(s + c^2)}} \tag{13}$$

Here $a, b$, and $c$ are the semiaxes of the ellipsoid and $N_a$ is the depolarization factor in the direction of the $a$-axis. For depolarization factors $N_b$ and $N_c$, interchange $b$ and $a$, and $c$ and $a$ in (13), respectively.

The three depolarization factors for any ellipsoid satisfy

$$N_a + N_b + N_c = 1 \tag{14}$$

This equality is also reflected in the unit-traceness property of the depolarization dyadic $\overline{\overline{L}}$. A sphere has three equal depolarization factors of 1/3. The other two special cases are a disc (depolarization

factors $1,0,0$), and a needle ($0,1/2,1/2$). For ellipsoids of revolution, prolate and oblate ellipsoids, closed-form expressions for the integral (13) can be found, and are given, for example in [13]. For a general ellipsoid with three different axes, the depolarization factors have to be calculated from the integral. Osborn and Stoner have tabulated the depolarization factors of a general ellipsoid [14–15].

Consider a mixture where all the ellipsoidal scatterers are of the same form and in aligned orientation, i.e. their corresponding axial directions are the same. This makes the mixture anisotropic. From (5), the exciting field in the direction of the $i$th axis is

$$\overline{E}^e = \overline{E} + N_i \frac{\overline{P}}{\epsilon_0} \tag{15}$$

and, if the polarizability of the scatterer is $\alpha_i$ in this direction, the effective permittivity component is

$$\epsilon_{\text{eff}}^i = \epsilon_0 + \frac{n\alpha_i}{1 - N_i \frac{n\alpha_i}{\epsilon_0}} \tag{16}$$

and the dyadic effective permittivity

$$\overline{\overline{\epsilon}}_{\text{eff}} = \epsilon_{\text{eff}}^x \hat{x}\hat{x} + \epsilon_{\text{eff}}^y \hat{y}\hat{y} + \epsilon_{\text{eff}}^z \hat{z}\hat{z} \tag{17}$$

If the ellipsoidal scatterers that have polarizability components $\alpha_x, \alpha_y$, and $\alpha_z$ are randomly oriented in the mixture, the material is isotropic and the effective permittivity scalar. In this case the average polarization has to be calculated by averaging over the dipole moments in different directions (see [1]), and the resulting effective permittivity is

$$\epsilon_{\text{eff}} = \epsilon_0 + \frac{\frac{1}{3}\sum_{i=x,y,z} n\alpha_i}{1 - \frac{1}{3}\sum_{i=x,y,z} N_i \frac{n\alpha_i}{\epsilon_0}} \tag{18}$$

There are also cases where the mixture may consist of scatterers with an orientation distribution that is not random or aligned as in these two extreme cases but describable rather by a number density $n(\Omega)$ as a function of three orientation angles. The average polarization depends on this distribution function and can be taken into account according to [1]. There sea ice is modeled with pure ice as the background,

and scatterers of spherical air bubbles and prolate needle-shaped brine pockets whose orientation distribution is Gaussian.

The effective permittivity can be given as a function of the polarizability $\alpha$ for other shapes also: in [7], the source dyadic $\overline{\overline{L}}$ has been given for cube, cylinder, rectangular parallelepiped, and pill box, and for a general scatterer shape, it can be evaluated from an integral. However, the analysis is here restricted to spheres and ellipsoids because for these, the polarizability can be found in closed form.

## 3.3 Polarizability

Basically, there are two ways of solving the polarizability of an inclusion with permittivity $\epsilon(\overline{r})$ in a quasistatic field: from the internal, or the external field of the inclusion. The first way is to start with the definition of the dipole moment

$$\overline{p} = \int_V dV[\epsilon(\overline{r}) - \epsilon_0]\overline{E}(\overline{r}) \tag{19}$$

where $V$ is the inclusion volume and $\epsilon_0$ is the permittivity of the background material. On the other hand, the dipole moment, being the product of the polarizability and the exciting field, gives the polarizability, because for a single scatterer in unbounded homogeneous space, the exciting field is the same as the incident field, cf. (5) with scatterer density $n \to 0$. This "internal" approach of solving the polarizability requires solving the internal field $\overline{E}(\overline{r})$ of the inclusion.

The other possibility is to consider the external field outside the inclusion. When the inclusion is present in a constant field, it generates a perturbation field with an inverse cubic distance dependence. This perturbation is the static field of a dipole located in the center of the inclusion and, from the amplitude of this perturbation outside the inclusion, the strength of the equivalent dipole can be inferred. The dipole component of the solution for the potential outside the inclusion is of the form $D_0 r^{-2}\cos\theta$ where $r$ is the distance from the center of the sphere and $\theta$ is the angle between the position vector and the incident field, see Fig. 3.1. The amplitude $D_0$ determines the dipole moment

$$\overline{p} = 4\pi\epsilon_0 D_0 \hat{z} \tag{20}$$

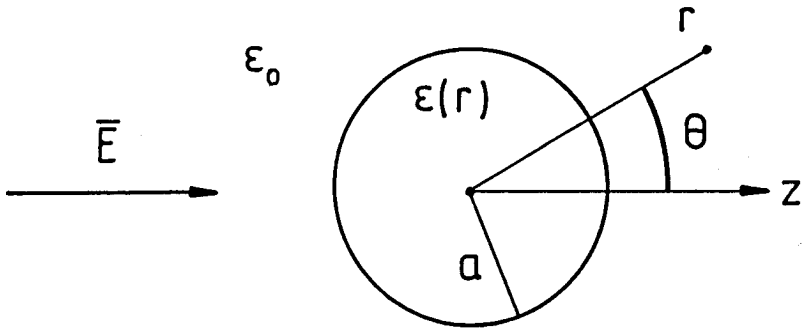


**Figure 3.1 Geometry of the problem: a polarizable inclusion in a static field.**

where $\hat{z}$ is the unit field direction vector. From the dipole moment, the polarizability results by dividing by the incident field amplitude $E$.

Naturally, both approaches, the internal and the external, lead to the same result. It depends on the functional form of the permittivity which way is more convenient in solving the dipole moment. Sometimes, interesting mathematical identities follow from the equivalence of the two solutions [4].

### *a. Homogeneous Scatterers*

In this section, the internal field approach is taken to solve the polarizability of homogeneous spherical and ellipsoidal scatterers.

#### *(1) Homogeneous Spheres*

Consider a homogeneous sphere of permittivity $\epsilon_1$ in unbounded homogeneous space of permittivity $\epsilon_0$. Let the radius of the sphere be $a_1$. It is well known [16] that if the sphere is subjected to a constant field of amplitude $\overline{E}$, the internal field $\overline{E}_{in}$ in the sphere is also

constant and of amplitude

$$\overline{E}_{in} = \overline{E}\frac{3\epsilon_0}{\epsilon_1 + 2\epsilon_0} \tag{21}$$

Therefore, from (19), the polarizability is equal to the product of the volume of the scatterer, its susceptibility, and the ratio between the inside and outside fields:

$$\alpha = \frac{4\pi a_1^3}{3}(\epsilon_1 - \epsilon_0)\frac{3\epsilon_0}{\epsilon_1 + 2\epsilon_0} \tag{22}$$

and the effective permittivity $\epsilon_{\text{eff}}$ of a mixture containing $n$ scatterers per unit volume of this type, is from (8)

$$\frac{\epsilon_{\text{eff}} - \epsilon_0}{\epsilon_{\text{eff}} + 2\epsilon_0} = f_1\frac{\epsilon_1 - \epsilon_0}{\epsilon_1 + 2\epsilon_0} \tag{23}$$

where $f_1 = n4\pi a_1^3/3$ is the volume fraction of the scatterer phase in the mixture. This equation is well known as the Rayleigh mixing formula and it can be written in the Maxwell-Garnett form [17]

$$\epsilon_{\text{eff}} = \epsilon_0 + 3\epsilon_0\frac{f_1\frac{\epsilon_1-\epsilon_0}{\epsilon_1+2\epsilon_0}}{1 - f_1\frac{\epsilon_1-\epsilon_0}{\epsilon_1+2\epsilon_0}} \tag{24}$$

### *(2) Homogeneous Ellipsoids*

If the scatterers are homogeneous and of ellipsoidal form, the internal field approach can be applied as in the spherical case, because the internal field is homogeneous also in this case. In the following, consider an incident field that is polarized along one of the axes of the ellipsoid. This entails no loss of generality because an oblique field can be resolved into components along the axes and the resultant polarizability is a superposition of the three component polarizabilities.

The polarizability of a homogeneous ellipsoid with permittivity $\epsilon_1$ and axes $a$, $b$, and $c$, in the direction of the $i$th axis is

$$\alpha_i = \frac{4\pi abc}{3}(\epsilon_1 - \epsilon_0)\frac{\epsilon_0}{\epsilon_0 + N_i(\epsilon_1 - \epsilon_0)} \tag{25}$$

where the depolarization factor $N_i$ is defined in (13). Hence, for a mixture of aligned ellipsoids with volume fraction $f_1$, the effective permittivity component in the $i$th direction is

$$\epsilon_{\text{eff}}^{i} = \epsilon_0 + \frac{\epsilon_0 f_1 \frac{\epsilon_1 - \epsilon_0}{\epsilon_0 + N_i(\epsilon_1 - \epsilon_0)}}{1 - f_1 \frac{N_i(\epsilon_1 - \epsilon_0)}{\epsilon_0 + N_i(\epsilon_1 - \epsilon_0)}} \tag{26}$$

and for a mixture with randomly oriented ellipsoids the scalar effective permittivity is

$$\epsilon_{\text{eff}} = \epsilon_0 + \frac{\frac{\epsilon_0 f_1}{3} \sum_{i=x,y,z} \frac{\epsilon_1 - \epsilon_0}{\epsilon_0 + N_i(\epsilon_1 - \epsilon_0)}}{1 - \frac{f_1}{3} \sum_{i=x,y,z} \frac{N_i(\epsilon_1 - \epsilon_0)}{\epsilon_0 + N_i(\epsilon_1 - \epsilon_0)}} \tag{27}$$

This ellipsoidal Maxwell-Garnett formula has been presented in many forms [18–21] and is discussed in [6].

In the formulae, the polarizability of a scatterer has been multiplied by the number density, resulting in a formula where only the volume fraction is visible. If in the ellipsoidal case there are different polarizabilities, like different permittivities or ellipsoids of different axial ratios, each of them gives one term (or three terms in the isotropic case) in the numerator and denominator of the effective permittivity expression, containing the volume fraction $f_i$ of this particular inclusion phase in the mixture. The modification is analogous to the transition from (8) to (9).

### *b. Multilayer Scatterers*

#### *(1) Multilayer Spheres*

Consider the case of calculating the polarizability of a multilayer sphere with radius $a_1$. This single inclusion is not homogeneous but its permittivity function is piecewise constant, each layer being dielectrically homogeneous according to Fig. 3.2. The boundary between subregions of permittivities $\epsilon_{i-1}$ and $\epsilon_i$ is a sphere with radius $a_i$. The number of layers is not limited.

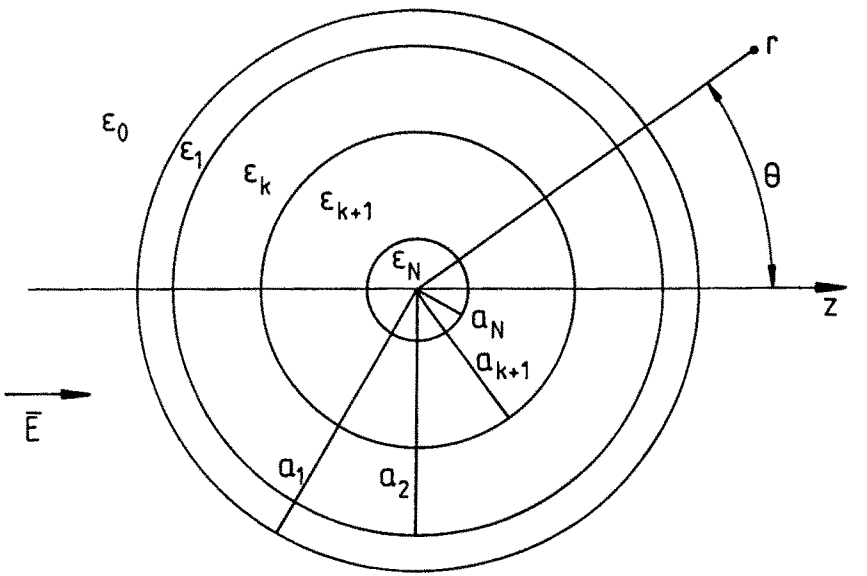


**Figure 3.2 A partially inhomogeneous dielectric sphere consisting of $N$ layers in a $z$-directed static field.**

To solve the dipole moment of this inclusion, the static problem of an incident field $\overline{E} = E\hat{z}$ permeating the space, i.e. the Laplace equation $\nabla^2\Phi(\bar{r}) = 0$ has to be solved for the potential $\Phi(\bar{r})$. The incident potential $-Er\cos\theta$ is that of a constant $z$-directed field of amplitude $E$. In each of the $N+1$ subregions of the problem, the $\theta$-dependence of the solution has to be $\cos\theta$ also because of the orthogonality of the Legendre polynomials. It is easy to show that the solution in the $i$th subregion is

$$\Phi_i(\bar{r}) = -C_i r\cos\theta + D_i r^{-2}\cos\theta \tag{28}$$

$C$ is the amplitude of the constant field component (the minus sign of this component leads to positive values for $C$ because the electric field is the negative gradient of the scalar potential and the incident field is polarized in the positive $z$-direction) and $D$ is the amplitude of the dipole type contribution to the field. Two of these $2N+2$ amplitudes are known: outside the sphere, which is the 0th region, the constant term is that of the incident field: $C_0 = E$. And in

the core region which includes the origin $r = 0$, the dipole term has to vanish: $D_N = 0$, because the field cannot reach infinite values.

Therefore, $2N$ unknowns are left. These can be solved from the $2N$ boundary conditions (the tangential electric field and the normal displacement have to be continuous at each of the $N$ boundaries) by inverting a $2N \times 2N$ matrix. Another method to solve the fields of the multilayer sphere, a transmission line analogy, has been presented in [3]. In that approach, the $C$ and $D$ fields are interpreted as inward and outward propagating fields, respectively, although there are no wave phenomena inside the inclusion. The boundary conditions connect the $C$ and $D$ fields in adjacent regions and these conditions can be described in propagation matrix form:

$$\begin{pmatrix} C_k \\ D_k \end{pmatrix} = \frac{1}{3\epsilon_k} \begin{pmatrix} \epsilon_{k+1} + 2\epsilon_k & 2(\epsilon_{k+1} - \epsilon_k)a_{k+1}^{-3} \\ (\epsilon_{k+1} - \epsilon_k)a_{k+1}^{3} & 2\epsilon_{k+1} + \epsilon_k \end{pmatrix} \begin{pmatrix} C_{k+1} \\ D_{k+1} \end{pmatrix} \tag{29}$$

The reflected $D$ fields are present everywhere except in the core region. This is because, after the forward-traveling field has reached the core, it continues to propagate towards the infinity of the origin and no more reflections occur. All field terms can be solved by the use of propagation matrices [22] and they depend on the layer permittivities and radii.

The dipole moment of one inclusion is easiest to calculate by using the external field approach because, in [3], a closed-form expression is given for the "reflection" from the multilayer sphere $D_0$:

$$D_0 = E \frac{(\epsilon_1 - \epsilon_0)a_1^3 + (2\epsilon_1 + \epsilon_0)\dfrac{(\epsilon_2-\epsilon_1)a_2^3+(2\epsilon_2+\epsilon_1)\frac{(\epsilon_3-\epsilon_2)a_3^3+\cdots}{(\epsilon_3+2\epsilon_2)+\cdots}}{(\epsilon_2+2\epsilon_1)+2(\epsilon_2-\epsilon_1)a_2^{-3}\frac{(\epsilon_3-\epsilon_2)a_3^3+\cdots}{(\epsilon_3+2\epsilon_2)+\cdots}}}{(\epsilon_1 + 2\epsilon_0) + 2(\epsilon_1 - \epsilon_0)a_1^{-3}\dfrac{(\epsilon_2-\epsilon_1)a_2^3+(2\epsilon_2+\epsilon_1)\frac{(\epsilon_3-\epsilon_2)a_3^3+\cdots}{(\epsilon_3+2\epsilon_2)+\cdots}}{(\epsilon_2+2\epsilon_1)+2(\epsilon_2-\epsilon_1)a_2^{-3}\frac{(\epsilon_3-\epsilon_2)a_3^3+\cdots}{(\epsilon_3+2\epsilon_2)+\cdots}}} \tag{30}$$

The numerators and denominators end with the term $\dfrac{D_{N-1}}{C_{N-1}}$

$$\frac{D_{N-1}}{C_{N-1}} = \frac{\epsilon_N - \epsilon_{N-1}}{\epsilon_N + 2\epsilon_{N-1}} a_N^3 \tag{31}$$

Hence, the dipole moment of the inclusion can be calculated according to (20).

If all the inclusions in the mixture are identical in structure, the ratios between the radii that appear in this expression can be expressed in terms of ratios between the volume fractions of the constituent components as follows

$$\frac{a_i^3}{a_j^3} = \frac{\sum_{l=i}^{N} f_l}{\sum_{l=j}^{N} f_l} \tag{32}$$

where $f_l$ is the volume fraction of material with permittivity $\epsilon_l$ in the mixture. Therefore, the effective permittivity of this mixture can be expressed in terms of the permittivities of the components and their volume fractions:

$$\frac{\epsilon_{\text{eff}} - \epsilon_0}{\epsilon_{\text{eff}} + 2\epsilon_0} = f \frac{(\epsilon_1 - \epsilon_0) + (2\epsilon_1 + \epsilon_0) \dfrac{(\epsilon_2 - \epsilon_1) a_2^3/a_1^3 + (2\epsilon_2 + \epsilon_1) \dfrac{(\epsilon_3 - \epsilon_2) a_3^3/a_1^3 + \cdots}{(\epsilon_3 + 2\epsilon_2) + \cdots}}{(\epsilon_2 + 2\epsilon_1) + 2(\epsilon_2 - \epsilon_1) \dfrac{(\epsilon_3 - \epsilon_2) a_3^3/a_2^3 + \cdots}{(\epsilon_3 + 2\epsilon_2) + \cdots}}}{(\epsilon_1 + 2\epsilon_0) + 2(\epsilon_1 - \epsilon_0) \dfrac{(\epsilon_2 - \epsilon_1) a_2^3/a_1^3 + (2\epsilon_2 + \epsilon_1) \dfrac{(\epsilon_3 - \epsilon_2) a_3^3/a_1^3 + \cdots}{(\epsilon_3 + 2\epsilon_2) + \cdots}}{(\epsilon_2 + 2\epsilon_1) + 2(\epsilon_2 - \epsilon_1) \dfrac{(\epsilon_3 - \epsilon_2) a_3^3/a_2^3 + \cdots}{(\epsilon_3 + 2\epsilon_2) + \cdots}}} \tag{33}$$

where $f$ is the total volume fraction of the inclusions. The relation between the dipole moment and polarizability gives

$$n a_1^3 = \frac{3}{4\pi} \sum_{l=1}^{N} f_l = \frac{3f}{4\pi} \tag{34}$$

The other way to calculate the dipole moment (the internal field approach) is to use (19), and integrate the product of the internal field and the susceptibility of the inclusion. In this approach, the field due to a potential of (28) has to be integrated over a spherical shell. From (28), two field types are generated. The $C$-field is a constant $z$-directed component and the integral is simply the product of its amplitude, the permittivity difference, and the volume of the shell. The other component is the $D$-field, or the dipole type field. However,

the integral of this field over a spherical homogeneous shell is zero as is shown in [4]. Therefore, the dipole moment is calculated from the $C$-field contribution in each subregion:

$$\overline{p} = \sum_{l=1}^{N} v_l(\epsilon_l - \epsilon_0)C_l\hat{z} \tag{35}$$

Here, $v_l$ denotes the volume of the shell with permittivity $\epsilon_l$.

The simplest mixture is two-phase, with background material of permittivity $\epsilon_0$ and inclusion permittivity $\epsilon_1$. The inclusions occupy the fraction $f_1$ in the mixture. From (33), the Rayleigh mixing formula (23) follows directly.

For the three-component mixture (where $N = 2$), the effective permittivity follows from (33):

$$\frac{\epsilon_{\text{eff}} - \epsilon_0}{\epsilon_{\text{eff}} + 2\epsilon_0} = (f_1 + f_2)\frac{(\epsilon_1 - \epsilon_0)(\epsilon_2 + 2\epsilon_1) + \frac{a_2^3}{a_1^3}(\epsilon_2 - \epsilon_1)(\epsilon_0 + 2\epsilon_1)}{(\epsilon_1 + 2\epsilon_0)(\epsilon_2 + 2\epsilon_1) + 2\frac{a_2^3}{a_1^3}(\epsilon_2 - \epsilon_1)(\epsilon_1 - \epsilon_0)} \tag{36}$$

This generalized Rayleigh mixing formula can be given also as

$$\frac{\epsilon_{\text{eff}} - \epsilon_0}{\epsilon_{\text{eff}} + 2\epsilon_0} = (f_1 + f_2)\frac{f_1(\epsilon_1 - \epsilon_0) + f_2 t_{12}(\epsilon_2 - \epsilon_0)}{f_1(\epsilon_1 + 2\epsilon_0) + f_2 t_{12}(\epsilon_2 + 2\epsilon_0)} \tag{37}$$

where

$$t_{12} = \frac{3\epsilon_1}{\epsilon_2 + 2\epsilon_1} \tag{38}$$

This formula is easily seen to give the two-phase mixing formula as the limit when $f_1 = 0$, $f_2 = 0$, $\epsilon_2 = \epsilon_1$, or $\epsilon_1 = \epsilon_0$. The same formula has been derived in [2] through the approach of calculating the internal fields in the core and the shell.

This formula can be compared to another three-phase mixing formula: to the case where the three phases are uncorrelated: the background material is still $\epsilon_0$ but the inclusions are homogeneous spheres and there are two types of them: spheres with permittivity $\epsilon_1$ and $\epsilon_2$ with volume fractions $f_1$ and $f_2$, respectively. The Rayleigh type representation for this mixture is

$$\frac{\epsilon_{\text{eff}} - \epsilon_0}{\epsilon_{\text{eff}} + 2\epsilon_0} = f_1\frac{\epsilon_1 - \epsilon_0}{\epsilon_1 + 2\epsilon_0} + f_2\frac{\epsilon_2 - \epsilon_0}{\epsilon_2 + 2\epsilon_0} \tag{39}$$

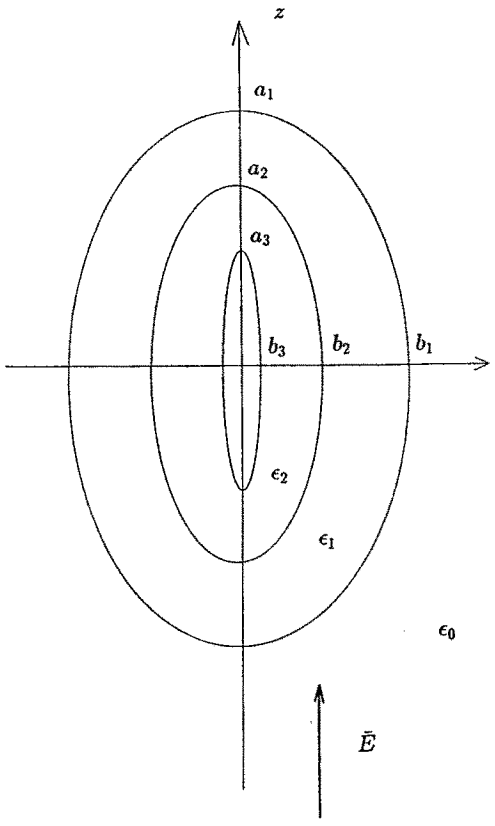


**Figure 3.3 A multilayer ellipsoid in a static field.**

For the explicit form of the four-component multilayer Rayleigh mixing formula ( $N = 3$ ), see [4].

### *(2) Multilayer Ellipsoids*

A mixture where the scatterers are multilayer ellipsoids can be treated in a more complicated but basically similar way. The field components and the polarizability can be obtained through transmission line analogy as in the spherical case. This is performed in detail in [5] and here only the results are given.

Consider a multilayer ellipsoid shown in Fig. 3.3 in a static $z$-directed field $\overline{E}$. The limitation of the form of the scatterer is that the boundaries have to be confocal ellipsoids. This is due to the re-

quirement that these boundaries be constant-coordinate surfaces in the ellipsoidal coordinate system, and entails that the outer ellipsoids of the scatterer are more spherical than the inner ones. The confocality restricts the ellipsoidal axes by

$$a_i^2 - a_j^2 = b_i^2 - b_j^2 = c_i^2 - c_j^2 \tag{40}$$

for all pairs $i, j$. In each subregion, the solution of the Laplace equation can be written as (see [5], [13], [23])

$$\Phi_i(\bar{r}) = -z\left[C - \frac{D}{2}\int_{\xi}^{\infty} \frac{ds}{(s+a_1^2)\sqrt{(s+a_1^2)(s+b_1^2)(s+c_1^2)}}\right] \tag{41}$$

where $a_1$, $b_1$, and $c_1$ are the semiaxes of the whole scatterer ellipsoid separating permittivities $\epsilon_1$ and $\epsilon_0$, and $a_1$ is the axis in the incident field direction ($z$). The coefficient of the $D$ solution is chosen to preserve conformity with the multilayer sphere problem. $\xi$ is an ellipsoidal coordinate and a constant $\xi$ defines an ellipsoidal surface.

From the boundary conditions, the transmission matrices connecting the adjacent potential amplitudes can be written

$$\begin{pmatrix} C_k \\ D_k \end{pmatrix} = \frac{1}{\epsilon_k} \begin{pmatrix} \epsilon_k + N_{k+1}^z(\epsilon_{k+1} - \epsilon_k) & \frac{N_{k+1}^z(1-N_{k+1}^z)}{a_{k+1}b_{k+1}c_{k+1}}(\epsilon_{k+1} - \epsilon_k) \\ a_{k+1}b_{k+1}c_{k+1}(\epsilon_{k+1} - \epsilon_k) & \epsilon_{k+1} + N_{k+1}^z(\epsilon_k - \epsilon_{k+1}) \end{pmatrix} \begin{pmatrix} C_{k+1} \\ D_{k+1} \end{pmatrix} \tag{42}$$

where $N_k^z$ is the depolarization factor in $z$-direction of the ellipsoid with semiaxes $a_k$, $b_k$, and $c_k$. As before, the reflection coefficient $D_0$ and from that the $z$-component of the polarizability $\alpha_z$ of the scatterer can be calculated:

$$\frac{n\alpha_z}{\epsilon_0} = f\frac{A}{B}$$

where

$$A = (\epsilon_1 - \epsilon_0) + [\epsilon_1 + N_1^z(\epsilon_0 - \epsilon_1)]$$

$$\frac{(\epsilon_2-\epsilon_1)\frac{V_2}{V_1}+[\epsilon_2+N_2^z(\epsilon_1-\epsilon_2)]\frac{(\epsilon_3-\epsilon_2)\frac{V_3}{V_1}+\cdots}{[\epsilon_2+N_3^z(\epsilon_3-\epsilon_2)]+\cdots}}{[\epsilon_1+N_2^z(\epsilon_2-\epsilon_1)]+N_2^z(1-N_2^z)(\epsilon_2-\epsilon_1)\frac{(\epsilon_3-\epsilon_2)\frac{V_3}{V_2}+\cdots}{[\epsilon_2+N_3^z(\epsilon_3-\epsilon_2)]+\cdots}}$$

$$B=[\epsilon_0+N_1^z(\epsilon_1-\epsilon_0)]+N_1^z(1-N_1^z)(\epsilon_1-\epsilon_0)\frac{(\epsilon_2-\epsilon_1)\frac{V_2}{V_1}+[\epsilon_2+N_2^z(\epsilon_1-\epsilon_2)]\frac{(\epsilon_3-\epsilon_2)\frac{V_3}{V_1}+\cdots}{[\epsilon_2+N_3^z(\epsilon_3-\epsilon_2)]+\cdots}}{[\epsilon_1+N_2^z(\epsilon_2-\epsilon_1)]+N_2^z(1-N_2^z)(\epsilon_2-\epsilon_1)\frac{(\epsilon_3-\epsilon_2)\frac{V_3}{V_2}+\cdots}{[\epsilon_2+N_3^z(\epsilon_3-\epsilon_2)]+\cdots}} \tag{43}$$

Here, $f$ is the volume fraction of the inclusions (the ratio of the inclusion volume to the total volume)

$$f=n\frac{4\pi}{3}a_1b_1c_1 \tag{44}$$

and $V_k$ is the volume of the ellipsoid inside the boundary between permittivities $\epsilon_{k-1}$ and $\epsilon_k$:

$$V_k=\frac{4\pi}{3}a_kb_kc_k \tag{45}$$

and the volume ratios can be expressed in terms of the volume fractions of the inclusions phases $f_i$. The equation (43) can be seen to give the multilayer sphere polarizability as the special case $N_i^z=1/3$. The effective permittivity for the isotropic and anisotropic mixtures result through the use of (18) and (17).

### *c. Continuous Permittivity Profile*

Mixtures can also be treated that contain inclusions of continuously inhomogeneous permittivity. This is the limit case of the multilayer scatterers analyzed in the previous section, i.e. the permittivity function of the scatterer must depend only on one coordinate.

The external field approach is most applicable in this case. The idea is to solve the differential equation for the scattered potential due to the dipole moment of the scatterer, and from the amplitude of this function, the polarizability can be calculated.

*(1) Inhomogeneous Spheres*

For the case of a spherical scatterer with a continuous permittivity profile, the permittivity function can only be a function of the distance from the center of the sphere: $\epsilon(\overline{r}) = \epsilon(r)$. Define the scattered field $-\nabla\Phi_s$ to be the difference between the total field $-\nabla\Phi$ (the field in the presence of the inclusion) and the $z$-directed incident field $\overline{E}$:

$$\nabla\Phi_s(\overline{r}) = \overline{E} + \nabla\Phi(\overline{r}) \tag{46}$$

The divergencelessness of the displacement, $\nabla \cdot \overline{D} = \nabla \cdot [-\epsilon(\overline{r})\nabla\Phi(\overline{r})] = 0$, leads to the following equation

$$\nabla \cdot [\epsilon(r)\nabla\Phi_s(\overline{r})] = \nabla\epsilon(r) \cdot \overline{E} = E\epsilon'(r)\cos\theta \tag{47}$$

Peeling off the $\theta$ dependence of the scattered potential, $\Phi_s(\overline{r}) = f_s(r)\cos\theta$, the following differential equation can be written for the $r$ dependence of the scattered potential

$$[\epsilon(r)r^2 f_s']' - 2\epsilon f_s = r^2 E\epsilon'(r) \tag{48}$$

The solution of this equation inside the inclusion ($0 \leq r \leq a$ where $a$ is the radius of the inclusion) depends on the permittivity profile. However, outside the inclusion (where $\epsilon'(r) = 0$), the scattered potential is easily seen to be of the form

$$\Phi_s(\overline{r}) = D_0 r^{-2}\cos\theta \tag{49}$$

The continuity of the scattered potential requires $D_0 = a^2 f_s(a)$. Not only the scattered potential but also its radial derivative has to be continuous at $r = a$ provided that the permittivity function matches the background permittivity at the boundary; then also the normal displacement is continuous as it should. As can be seen from (48), the scattered potential vanishes in the origin. It increases with $r$, and decays outside the inclusion.

For enumerating the effective permittivity of mixtures with this type of inclusions, the only quantity that is needed in the external approach is the amplitude of the scattered field at the boundary. $a^2 f_s(a)$ equals the dipole amplitude $D_0$ as before which gives the dipole moment according to (20).

The equation (48) can be solved in power series form given the Taylor series of the inclusion permittivity profile. Let the permittivity function be expanded

$$\epsilon(r) = \sum_{k=0}^{\infty} \epsilon_k \left(\frac{r}{a}\right)^k \tag{50}$$

The equation (48) has a regular singular point at $r = 0$ (see [24]). Substituting a Frobenius series in the equation

$$f_s(r) = Ea(\tfrac{r}{a})^\beta \sum_{k=0}^{\infty} a_k (\tfrac{r}{a})^k$$

it can be seen that $\beta$ is integer and the solution is analytic at $r = 0$. Choosing $\beta = 0$, the coefficients $a_k$ can be calculated:

$$\begin{aligned}
a_0 &= 0 \\
a_1 &= c \\
4\epsilon_0 a_2 &= \epsilon_1 - \epsilon_1 a_1 \\
10\epsilon_0 a_3 &= 2\epsilon_2 - 6\epsilon_1 a_2 - 2\epsilon_2 a_1 \\
18\epsilon_0 a_4 &= 3\epsilon_3 - 13\epsilon_1 a_3 - 8\epsilon_2 a_2 - 3\epsilon_3 a_1 \\
28\epsilon_0 a_5 &= 4\epsilon_4 - 22\epsilon_1 a_4 - 16\epsilon_2 a_3 - 10\epsilon_3 a_2 - 4\epsilon_4 a_1 \\
(k+2)(k-1)\epsilon_0 a_k &= (k-1)\epsilon_{k-1} + \sum_{m=1}^{k-1} [2 - m(k+1)]\epsilon_{k-m} a_m \\
& \qquad k > 1
\end{aligned} \tag{52}$$

Here, the linear term $a_1 = c$ is arbitrary and is determined from the boundary conditions: matching the function and its derivative to the dipole potential outside the inclusion.

The recursion for the general term can also be written in the following compact form

$$(k-1)\epsilon_{k-1} = \sum_{m=1}^{k} [m(k+1) - 2]\epsilon_{k-m} a_m \tag{53}$$

As the coefficients $a_k$ are solved, the polarizability can be calculated

$$\alpha = \frac{4\pi\epsilon_0}{E} a^2 f_s(a) = 4\pi\epsilon_0 a^3 \sum_{k=0}^{\infty} a_k \tag{54}$$

Again, from the polarizability, the effective permittivity is found.

Consider the scattered field of a sphere with the following linear permittivity profile (the permittivity decreases linearly from the core value $\epsilon_c$ to the background value)

$$\epsilon(r) = \epsilon_c - \Delta\epsilon \frac{r}{a} \qquad 0 \le r \le a \tag{55}$$

$$\epsilon(r) = \epsilon_c - \Delta\epsilon = \epsilon_0 \qquad r \ge a \tag{56}$$

The Taylor-series solution for the scattered potential is

$$f_s(r) = Ea \sum_{k=0}^{\infty} b_k \left(\frac{r}{a}\right)^k$$

with

$$\begin{aligned}
b_0 &= 0 \\
b_1 &= c \\
b_2 &= -\frac{1}{4}\frac{\Delta\epsilon}{\epsilon_c}(1 - b_1) \\
b_3 &= \frac{6}{10}\frac{\Delta\epsilon}{\epsilon_c} b_2 \\
b_4 &= \frac{13}{18}\frac{\Delta\epsilon}{\epsilon_c} b_3 \\
b_k &= \frac{k^2 - 3}{(k+2)(k-1)}\frac{\Delta\epsilon}{\epsilon_c} b_{k-1} \qquad k > 2
\end{aligned} \tag{57}$$

The dipole moment amplitude comes from

$$f_s(a) = Ea \sum_{k=0}^{\infty} b_k \tag{58}$$

For a sphere with parabolically decreasing permittivity

$$\epsilon(r) = \epsilon_c - \Delta\epsilon \left(\frac{r}{a}\right)^2 \qquad 0 \le r \le a \tag{59}$$

$$\epsilon(r) = \epsilon_c - \Delta\epsilon = \epsilon_0 \qquad r \ge a \tag{60}$$

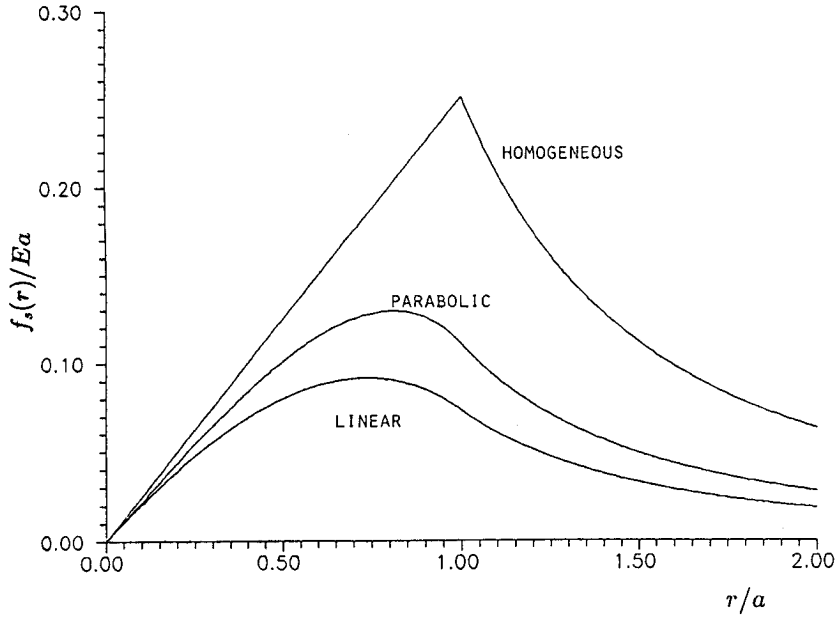


**Figure 3.4 The scattered potential function $f_s(r)$ in the neighborhood of spheres with homogeneous,linear, and parabolic permittivity profiles. The core-to-background permittivity ratio is 2 for each scatterer.**

The Taylor-series solution for the scattered potential is

$$f_s(r) = Ea \sum_{k=0}^{\infty} c_k \left(\frac{r}{a}\right)^k$$

with

$$\begin{aligned} c_0 &= 0 \\ c_1 &= c \\ c_2 &= 0 \\ c_3 &= -\frac{1}{5}\frac{\Delta\epsilon}{\epsilon_c}(1 - c_1) \\ c_4 &= 0 \\ c_5 &= \frac{4}{7}\frac{\Delta\epsilon}{\epsilon_c}c_3 \end{aligned}$$

$$c_{k+2} = \frac{k^2 + 3k - 2}{(k+1)(k+4)} \frac{\Delta\epsilon}{\epsilon_c} c_k \qquad k > 1 \tag{61}$$

The scattered potential is an odd function of $r$. The free parameter $c$ is determined as before from the boundary conditions. The dipole moment amplitude comes from

$$f_s(a) = Ea \sum_{k=0}^{\infty} c_k \tag{62}$$

From a numerical point of view, the series converges fairly quickly: for the case $\epsilon_c/\epsilon_0 = 2$, only seven terms are needed in the series to produce 1% accuracy in the polarizability $\alpha$. It is worth noting that as the core-background permittivity contrast increases, the series converges more slowly: for the case $\epsilon_c/\epsilon_0 = 10$, about five times as many terms are needed than for $\epsilon_c/\epsilon_0 = 1.5$ in order to get the same accuracy.

Figure 3.4 shows the scattered potential function $f_s(r)$ for homogeneous, linear, and parabolic permittivity profiles with permittivity ratios $\epsilon_c/\epsilon_0 = 2$. The discontinuity of the derivative of the homogeneous sphere is due to the discontinuity of the permittivity function at that point.

*(2) Inhomogeneous Ellipsoids*

Also the ellipsoidal scatterer with continuous permittivity profile can be attacked. This case is the limit of the process of increasing the number of layers in a multilayer ellipsoid and making these thinner at the same time. Naturally, the permittivity profile of the continuously inhomogeneous ellipsoid cannot be arbitrary but be only dependent on the $\xi$ coordinate of the ellipsoidal coordinate system:

$$\epsilon(\bar{r}) = \epsilon(\xi) \tag{63}$$

As in the spherical case, the polarizability or the dipole moment of the ellipsoid in a static field can be calculated from the scattered potential, the dipole term of the solution of the Laplace equation outside the scatterer.

Let the incident uniform field be $z$-directed, as before. The total field outside and inside the scatterer $-\nabla\Phi$ is the sum of the incident

field $\overline{E}$ and the scattered field $-\nabla\Phi_s$ where $\Phi_s$ is the scattered potential, the amplitude of which is proportional to the dipole moment of the scatterer.

The divergencelessness of the displacement leads in this case to the following equation

$$\nabla \cdot [\epsilon(\xi)\nabla\Phi_s(\overline{r})] = \nabla\epsilon(\xi) \cdot \overline{E} = E\hat{z} \cdot \nabla\epsilon(\xi) \tag{64}$$

where $\hat{z}$ is the unit vector in $z$ direction. As before (equation (41)), from the scattered potential, $z$ has to be peeled off in order for the rest to be only a function of $\xi$:

$$\phi_s(\overline{r}) = zf_s(\xi) \tag{65}$$

Performing the differential operations in ellipsoidal coordinates, it can be seen after some algebra (see [5]) that the dependencies other than $\xi$ cancel from the differential equation (64), the resulting equation for the $\xi$-dependent scattered potential being

$$2(\xi + a^2)\epsilon(\xi)f_s''(\xi) + \left[3 + \frac{\xi + a^2}{\xi + b^2} + \frac{\xi + a^2}{\xi + c^2}\right]\epsilon(\xi)f_s'(\xi)$$

$$+2(\xi + a^2)\epsilon'(\xi)f_s'(\xi) + \epsilon'(\xi)f_s(\xi) = \epsilon'(\xi)E \tag{66}$$

where $a, b$, and $c$ are the axes of the ellipsoid in $z, x$, and $y$ directions, respectively. This second-order ordinary differential equation for the unknown function $f_s(\xi)$ can also be written in the form

$$\left[\epsilon(\xi)(\xi + a^2)R(\xi)f_s'(\xi)\right]' + \epsilon'(\xi)\frac{R(\xi)}{2}f_s(\xi) = \epsilon'(\xi)\frac{R(\xi)}{2}E \tag{67}$$

where $R(\xi) = \sqrt{(\xi + a^2)(\xi + b^2)(\xi + c^2)}$. As before (equation (41)), the surface of the scatterer is the $\xi = 0$ surface. $\xi$ is negative inside the ellipsoid and positive outside it. On the $z$ axis, the connection between the coordinates is $z^2 = \xi + a^2$. The smallest value for $\xi$ is $-d^2$ where $d$ is the smallest of the three axes $a, b$, and $c$. The core of the ellipsoid, i.e. the surface where $\xi$ has the minimum value, is an ellipse in the plane of the two major axes of the ellipsoid, and this ellipse shrinks to a point as the ellipsoid degenerates into a sphere.

Given the permittivity profile $\epsilon(\xi)$, the solution can be found in a similar way as in the spherical case. From the amplitude of the scattered field outside the ellipsoid, when $\xi > 0$, the polarizability in the

$z$ direction, $\alpha_z$ can be calculated. The dipole moment and the polarizability in this direction are given by the scattered field amplitude $D_0$. Its connection to the amplitude of the $f_s$ function is

$$f_s(0) = E\frac{D_0}{2}\int_0^\infty \frac{ds}{(s+a^2)R(s)} = ED_0\frac{N_z}{abc} \tag{68}$$

where $N_z$ is the depolarization factor of the ellipsoid in the $z$ direction. Hence, the polarizability is

$$\alpha_z = \frac{\epsilon_0 V}{N_z E} f_s(0) \tag{69}$$

Knowing this, and the corresponding polarizability components in the $x$ and $y$ directions, the anisotropic and isotropic effective permittivities of mixtures containing this type of scatterers (in aligned orientation and randomly oriented, respectively) can be calculated using expressions (17) and (18).

### *d. Variational Method for Solving the Polarizability*

In this section, a variational method is presented for calculating the polarizability. The focus is on spherical scatterers but a variational principle can be derived for the ellipsoidal case as well.

In modeling geophysical materials in nature, it is useful to be able to calculate the effective permittivity of random media with permittivity fluctuations that follow a Gaussian dependence instead of a bounded permittivity function. The differential equation (48) for $f_s$, though still perfectly valid, is not anymore suitable for solving the polarizability because there is no precise boundary between the inclusion and the background medium. Hence, the accuracy achieved in a closed interval of the previous section cannot be realized. This is because in this case the Frobenius series has to apply in the whole semi-infinite range beyond the "boundary" $r = a$ (the permittivity perturbation has not yet reached the background value). However, in numerical calculations, the series has to be truncated and a truncated power series diverges, whence it is difficult to satisfy the boundary condition at infinity. Therefore, a different approach has to be taken.

The variational method has been shown to be an efficient tool in solving problems where only one parameter of the problem is of interest [25–26]. By exploiting stationary property functionals derivable

from eigenvalue equations, accurate estimates for this parameter can be calculated because its error is of second order if the error in trial fields is of first order.

In the problem under consideration, an inclusion in a constant field $\overline{E}$, advantage can be taken from the energy functional. Consider the differential equation

$$\nabla \cdot (\epsilon \nabla \Phi_s) = [\nabla(\epsilon - \epsilon_0)] \cdot \overline{E} \tag{70}$$

for the unknown scattered potential $\Phi_s(\bar{r})$. This is of the form

$$Lf = g \tag{71}$$

where $L$ is the linear differential operator and $g$ is the known function. The energy functional for this deterministic problem is

$$J(f) = \int f\, Lf\, dV - 2 \int f\, g\, dV \tag{72}$$

The operator is self-adjoint and the integrations extend to infinity where the scattered potential vanishes fast enough not to create any surface terms. The stationary value of the energy functional is

$$J_{\text{stat}} = -\int f\, g\, dV = -\int \Phi_s [\nabla(\epsilon - \epsilon_0)] \cdot \overline{E}\, dV \tag{73}$$

where $\overline{E}$ is the incident constant field. Integration by parts gives

$$\begin{aligned} J_{\text{stat}} &= \int (\epsilon - \epsilon_0) \nabla \Phi_s \cdot \overline{E}\, dV \\ &= |\overline{E}|^2 \int (\epsilon - \epsilon_0) dV - \int (\epsilon - \epsilon_0)(\overline{E} - \nabla \Phi_s) \cdot \overline{E}\, dV \end{aligned} \tag{74}$$

The last integral can be related with the polarizability of the inclusion because the total field is the incident plus the scattered field $\overline{E} - \nabla \Phi_s$ and $\overline{E}$ is constant. Therefore,

$$J_{\text{stat}} = -\alpha |\overline{E}|^2 + |\overline{E}|^2 \int (\epsilon - \epsilon_0) dV \tag{75}$$

Hence, a new functional can be written which has the polarizability $\alpha$ as a stationary point:

$$J(\Phi_s) = \int (\epsilon - \epsilon_0) dV + \frac{1}{|\overline{E}|^2} \left[ - \int \Phi_s \nabla \cdot (\epsilon \nabla \Phi_s) dV + 2 \int \Phi_s \nabla (\epsilon - \epsilon_0) \cdot \overline{E} dV \right] \quad (76)$$

Integration by parts gives

$$J(\Phi_s) = \int (\epsilon - \epsilon_0) dV + \frac{1}{|\overline{E}|^2} \left[ \int \epsilon |\nabla \Phi_s|^2 dV + 2 \int \Phi_s \nabla (\epsilon - \epsilon_0) \cdot \overline{E} dV \right] \quad (77)$$

This functional is dependent on the amplitude of the function $\Phi_s$. An amplitude-independent functional is more efficient in estimating the polarizability and can be derived by setting $\Phi_s = A\Psi_s$ and searching analytically the amplitude $A$ giving the extreme value of the functional. This gives the functional

$$J(\Psi_s) = \int (\epsilon - \epsilon_0) dV - \frac{1}{|\overline{E}|^2} \frac{\left( \int \Psi_s \nabla \epsilon \cdot \overline{E} dV \right)^2}{\int \epsilon (\nabla \Psi_s)^2 dV} \quad (78)$$

For inclusions with spherically symmetric permittivity profile and the scattered field function as

$$\Psi_s(\overline{r}) = f_s(r) \cos\theta \quad (79)$$

the functional simplifies to

$$J(f_s) = 4\pi \int_0^\infty r^2 [\epsilon(r) - \epsilon_0] dr - \frac{4\pi}{3} \frac{\left[ \int_0^\infty r^2 f_s(r) \epsilon'(r) dr \right]^2}{\int_0^\infty \epsilon(r) \left[ r^2 f_s'^2(r) + 2 f_s^2(r) \right] dr} \quad (80)$$

If the inclusion is bounded within a region $r \leq a$, the upper limit is $a$ in the first integral and in the numerator integral of the second term.

A check for the functional is to calculate the polarizability of a homogeneous sphere with radius $a$ and permittivity $\epsilon_1$. The scattered field is $f_s(r) = r$ inside the sphere and $f_s(r) = a^3/r^2$ outside the sphere. Also, $\epsilon'(r) = -(\epsilon_1 - \epsilon_0)\delta(a)$. After performing the integrations,

$$J_{\text{stat}} = \alpha = \frac{4\pi}{3} a^3 (\epsilon_1 - \epsilon_0) \frac{3\epsilon_0}{\epsilon_1 + 2\epsilon_0} \tag{81}$$

which is correct.

The functional can be used to estimate the polarizability of a given scatterer. In [4] it is shown that with a simple parabolic trial function for the scattered potential of a, the polarizability from the functional has an error of only 1 %.

The variational method is probably the most efficient way to attack the problem of calculating the polarizability of Gaussian packets, i.e. inclusions with the following exponential permittivity profile

$$\epsilon(r) = \epsilon_0 + \Delta\epsilon \exp[-(r/a)^2] \tag{82}$$

There is no boundary between the inclusion and the background material, and the integrations in the functional extend to infinity. In [4], the polarizability of Gaussian packets is solved through the variational approach. There also an interesting comparison is made between scatterers of different permittivity profiles. The problem studied is, which functional form the permittivity profile should have in order to produce a maximum polarizability and dipole moment, and, consequently, the largest effective permittivity, provided that the "dielectric mass" remains the same. The "dielectric mass" $m_\epsilon$ is the susceptibility integral over the inclusion volume

$$m_\epsilon = \int_V [\epsilon(\bar{r}) - \epsilon_0] dV \tag{83}$$

The result is that with equal $m_\epsilon$, the polarizabilities fall in the following order:

$$\alpha_{\text{Gaussian}} > \alpha_{\text{linear}} > \alpha_{\text{parabolic}} > \alpha_{\text{homogeneous}} \tag{84}$$

The same order applies to the effective permittivity of mixtures containing these types of inclusions.

## 3.4 Dense and Scattering Mixtures

### *a. Apparent Permittivity*

In previous derivations, the dipole moment and the polarizability of a single inclusion was calculated from the macroscopic field adding to it the average polarization resulting from dipole moments in the neighborhood of the scatterer. So far the amplitude ratio between the inside and outside fields (that is needed in the internal field approach) was calculated assuming the scatterer to be embedded in infinite homogeneous background material of the permittivity $\epsilon_0$ as was also the case when determining the cavity field from the permeating polarization. This may be a good approximation for sparse mixtures. However, for cases where the scatterers are more densely packed, the dielectric constant "seen" outside the scatterer is different from that of the host medium. In the following, this dielectric constant will be called the *apparent permittivity* $\epsilon_a$.

The modifications in equations (5) and (25) necessary in incorporating the apparent permittivity are

$$\overline{E}^e = \overline{E} + \frac{1}{\epsilon_a}\overline{\overline{L}} \cdot \overline{P} \tag{85}$$

$$\alpha_i = \frac{4\pi abc}{3}(\epsilon_1 - \epsilon_0)\frac{\epsilon_a}{\epsilon_a + N_i(\epsilon_1 - \epsilon_0)} \tag{86}$$

Therefore, the effective permittivity of a mixture with randomly oriented ellipsoidal inclusions, a generalization of equation (27) is

$$\epsilon_{\text{eff}} = \epsilon_0 + \frac{\frac{\epsilon_a f_1}{3}\sum_{i=x,y,z}\frac{\epsilon_1-\epsilon_0}{\epsilon_a+N_i(\epsilon_1-\epsilon_0)}}{1-\frac{f_1}{3}\sum_{i=x,y,z}\frac{N_i(\epsilon_1-\epsilon_0)}{\epsilon_a+N_i(\epsilon_1-\epsilon_0)}} \tag{87}$$

This can also be expressed in the form

$$\epsilon_{\text{eff}} = \epsilon_0 + \frac{f_1}{3}(\epsilon_1 - \epsilon_0)\sum_{i=x,y,z}\frac{\epsilon_a + N_i(\epsilon_{\text{eff}} - \epsilon_0)}{\epsilon_a + N_i(\epsilon_1 - \epsilon_0)} \tag{88}$$

from which it can be clearly seen that regardless of the choice of $\epsilon_a$, the formula gives $\epsilon_{\text{eff}} = \epsilon_1$, as $f_1 = 1$.

An intuitive choice for the apparent permittivity is that it equals some value between the host permittivity $\epsilon_0$ and the effective permittivity $\epsilon_{\text{eff}}$. This generally leads to a nonlinear, or implicit, equation for $\epsilon_{\text{eff}}$, but practice has shown that an iterative process will lead rapidly to a solution. Consider the following expression for $\epsilon_a$:

$$\epsilon_a = \epsilon_0 + a(\epsilon_{\text{eff}} - \epsilon_0) \tag{89}$$

where $a$ is a parameter. It is interesting to note that for small volume fraction values $f_1$, the effective permittivity $\epsilon_{\text{eff}}$ is independent of $a$ as can be seen from the perturbation expansion of equation (88):

$$\epsilon_{\text{eff}} = \epsilon_0 + \frac{f_1}{3}(\epsilon_1 - \epsilon_0) \sum_{i=x,y,z} \frac{\epsilon_0}{\epsilon_0 + N_i(\epsilon_1 - \epsilon_0)} + O(f_1^2) \tag{90}$$

Mätzler [27] has also noted the similarity of the linear term in certain mixing formulas nonlinear in the volume fraction dependence. For second- and third-order terms of spherical-inclusion mixing formulas, see [6]. With different choices for the parameter $a$, equation (88) reduces to some previously known mixing formulas. Naturally, for the choice $a = 0$, the generalized Maxwell-Garnett formula (27) is recaptured. With the value $a = 1$, and for spherical scatterers $N_i = 1/3$, the effective permittivity follows the formula

$$\epsilon_{\text{eff}} = \epsilon_0 + \frac{3f_1\epsilon_{\text{eff}}(\epsilon_1 - \epsilon_0)}{3\epsilon_{\text{eff}} + (1 - f_1)(\epsilon_1 - \epsilon_0)} \tag{91}$$

This is the low-frequency result of the "quasicrystalline approximation with coherent potential" formula that has been previously derived for spheres [28–29] and here it is generalized for ellipsoids. In solid state physics, QCA-CP is known as the GKM approximation after Gyorffy, Korringa, and Mills.

A compromise between these two choices $a = 0$ and $a = 1$, is $a = 1 - N_i$. This gives for the effective permittivity

$$\epsilon_{\text{eff}} = \epsilon_0 + \frac{f_1}{3}(\epsilon_1 - \epsilon_0) \sum_{i=x,y,z} \frac{\epsilon_{\text{eff}}}{\epsilon_{\text{eff}} + N_i(\epsilon_1 - \epsilon_{\text{eff}})} \tag{92}$$

which is widely known as the Polder - van Santen mixing formula and has been derived through other approaches than the one followed above

[29–33]. In the case of spherical scatterers ( $a = 2/3$ ), it is also referred to as the effective medium theory formula [28] or the Böttcher mixing formula [34]

$$\frac{\epsilon_{\text{eff}} - \epsilon_0}{3\epsilon_{\text{eff}}} = f_1 \frac{\epsilon_1 - \epsilon_0}{\epsilon_1 + 2\epsilon_{\text{eff}}} \tag{93}$$

In remote sensing applications, the Polder - van Santen formula has been used with success in explaining and predicting the dielectric behavior of dense geophysical media, snow and soil [35–37].

### *b. Other Mixing Formulae*

In the literature, there are also mixing formulae for the case of spherical scatterers that share the common trait of expressing a relation that contains one-third powers of the different permittivities. Three different formulas of this type have been presented: the Looyenga formula [38], the Bruggeman formula [39], and the formula by Sen, Scala, and Cohen [40]. The approach in deriving these formulas is differential: the excess polarization is calculated due to a small sphere, and by letting the sphere become infinitesimal, a differential equation results for the effective permittivity, the solution of which contains these fractional powers of a third.

The Looyenga formula reads

$$\epsilon_{\text{eff}}^{1/3} = f_1 \epsilon_1^{1/3} + (1 - f_1)\epsilon_0^{1/3} \tag{94}$$

It can be seen that the Looyenga formula is symmetric with respect to the two components; there is no difference which one of them is considered as host and which as inclusion. In [37], the Looyenga model is considered as a member of the family of exponential models, similar to, for example, the Birchak formula [41] where the 1/3-power of the Looyenga model is replaced by 1/2: the square roots of the permittivities add up to the square root of the effective permittivity. The Looyenga formula has been derived also by Landau and Lifshitz [13].

The Bruggeman formula is as follows

$$\frac{\epsilon_1 - \epsilon_{\text{eff}}}{\epsilon_1 - \epsilon_0} = (1 - f_1)\left(\frac{\epsilon_{\text{eff}}}{\epsilon_0}\right)^{1/3} \tag{95}$$

and the formula by Sen, Scala, and Cohen is the following

$$\frac{\epsilon_{\text{eff}} - \epsilon_0}{\epsilon_1 - \epsilon_0} = f_1 \left( \frac{\epsilon_{\text{eff}}}{\epsilon_1} \right)^{1/3} \tag{96}$$

These two models contain the effective permittivity implicitly. Its direct calculation requires solving a third-order equation. The Bruggeman model and the Sen-Scala-Cohen model can be seen to be complementary: if the background permittivity is changed to the inclusion permittivity and vice versa, and also their volume fractions ( $f_1 \to 1 - f_1$ ), the Bruggeman formula is converted to the Sen-Scala-Cohen formula and vice versa.

The effective permittivity calculated from these formulas, for cases of considerable inclusion-background permittivity contrast, is smallest according to the Bruggeman formula and biggest according to the model by Sen, Scala, and Cohen. The Looyenga mixing formula gives values that fall between these two. This can be seen explicitely from the three-term perturbation expansions in $f_1$ of these three formulas.

Looyenga:

$$\epsilon_{\text{eff}} = \epsilon_0 + f_1 \, 3\epsilon_0^{2/3}(\epsilon_1^{1/3} - \epsilon_0^{1/3}) + f_1^2 \, 3\epsilon_0^{1/3}(\epsilon_1^{1/3} - \epsilon_0^{1/3})^2 + \cdots \tag{97}$$

Bruggeman:

$$\epsilon_{\text{eff}} = \epsilon_0 + f_1 \, 3\epsilon_0 \frac{\epsilon_1 - \epsilon_0}{\epsilon_1 + 2\epsilon_0} + f_1^2 \, 3\epsilon_0 \left( \frac{\epsilon_1 - \epsilon_0}{\epsilon_1 + 2\epsilon_0} \right)^2 \frac{\epsilon_0 + 2\epsilon_1}{\epsilon_1 + 2\epsilon_0} + \cdots \tag{98}$$

Sen, Scala, and Cohen:

$$\epsilon_{\text{eff}} = \epsilon_0 + f_1 (\epsilon_1 - \epsilon_0) \left( \frac{\epsilon_0}{\epsilon_1} \right)^{1/3} + f_1^2 \frac{(\epsilon_1 - \epsilon_0)^2}{3\epsilon_0^{1/3}\epsilon_1^{2/3}} + \cdots \tag{99}$$

It is worth noting that the Bruggeman formula contains the same linear term as the formulas presented through introducing the apparent permittivity above. Comparison between the expansion of the Bruggeman formula and the perturbation expansion of the equation (88) reveals that up to second order in $f_1$, the Bruggeman formula agrees with the mixing formula (88), provided that the parameter value be $a = 1/3$. Hence, it seems that the formula (88) gives relevant mixing rules with all small positive $a$-values 0, 1/3, 2/3, and 1.

The Lichtenecker formula [42–43] volume-averages the natural logarithms of the permittivities:

$$\ln \epsilon_{\text{eff}} = (1 - f_1) \ln \epsilon_0 + f_1 \ln \epsilon_1 \tag{100}$$

It is interesting to see that the Lichtenecker formula belongs to the family of the exponential models as a limit case when the exponent decreases to zero. The exponential model of degree $n$ gives

$$\epsilon_{\text{eff}}^{1/n} = (1 - f_1)\epsilon_0^{1/n} + f_1 \epsilon_1^{1/n} \tag{101}$$

For $n \to \infty$, the Taylor expansion

$$\epsilon_i^{1/n} = \epsilon_i^0 + \frac{1}{n} \frac{\partial \epsilon_i^{1/n}}{\partial (1/n)} = 1 + \frac{1}{n} \ln \epsilon_i \tag{102}$$

shows that the effective permittivity is

$$\epsilon_{\text{eff}} = \left[ 1 + \frac{1}{n} \left( \ln \epsilon_0 + f_1 \ln \frac{\epsilon_1}{\epsilon_0} \right) \right]^n \tag{103}$$

which in the limit is the Lichtenecker formula because of the property of the exponential function [44]

$$e^z = \lim_{n \to \infty} \left( 1 + \frac{z}{n} \right)^n \tag{104}$$

Other presented mixing rules like the ones by Runge [45] and Meredith and Tobias [46] are discussed in [6] where also their results are compared. In this reference, the apparent permittivity and aspects of self-consistency are also discussed in the case of spherical multilayer scatterers. In previous literature, there are also a few analyses on mixtures with two-layer spheres and ellipsoidal shells [47–50].

### *c. Scattering Considerations*

In the case of mixtures with discrete inclusion particles, scattering phenomena have to be considered as the frequency increases. The first notable effect due to this is that the coherent wave propagating through the mixture will suffer attenuation that is greater than that following from pure absorption. In other words, the imaginary part of the effective permittivity of the heterogeneous medium will increase by an extra scattering term that is additive with the absorption term:

$$\epsilon''_{\text{eff}} = \epsilon''_{\text{eff,abs}} + \epsilon''_{\text{eff,sca}} \tag{105}$$

This scattering problem can be approached with the multiple scattering equations, and the scattering attenuation term can be evaluated by seeking approximative solutions to these multiple scattering equations. Different approaches to multiple scattering equations have been presented in [29], and the resulting formulas for the effective permittivity, which contain the most important scattering term, are as follows.

For spherical particles, the "effective field approximation" that is valid for sparse concentration of scatterers leads to the formula

$$\epsilon_{\text{eff}} = \epsilon_0 + 3\epsilon_0 f_1 \frac{\epsilon_1 - \epsilon_0}{\epsilon_1 + 2\epsilon_0} \left[ 1 + i\frac{2}{3}(ka)^3 \frac{\epsilon_1 - \epsilon_0}{\epsilon_1 + 2\epsilon_0} \right] \tag{106}$$

where $k = \omega\sqrt{\mu_0\epsilon_0}$ is the wave number and $a$ is the radius of the spherical scatterers. $ka$ is the size parameter of the scatterers. It can be seen that the scattering term is strongly frequency dependent, containing the third power of frequency, and for sufficiently small scatterers, it is negligible. On the other hand, this formula is approximative in the sense that it does not give the Maxwell-Garnett formula in the low-frequency limit. Anyway, for small volume fractions of the inclusion phase, it gives good results: for $f_1 = 0.05$, the error is less than 5%, depending on the inclusion permittivity. The sharper the contrast between the phases, the larger the error is. This can be remedied by using the quasicrystalline approximation [29], which gives an improvement over the previous formula:

$$\epsilon_{\text{eff}} = \epsilon_0 + 3\epsilon_0 f_1 \frac{\frac{\epsilon_1 - \epsilon_0}{\epsilon_1 + 2\epsilon_0}}{1 - f_1 \frac{\epsilon_1 - \epsilon_0}{\epsilon_1 + 2\epsilon_0}} \left\{ 1 + i\frac{2}{3}(ka)^3 \frac{\frac{\epsilon_1 - \epsilon_0}{\epsilon_1 + 2\epsilon_0}}{1 - f_1 \frac{\epsilon_1 - \epsilon_0}{\epsilon_1 + 2\epsilon_0}} \left[ 1 + 4\pi n \int_0^\infty r^2 [g(r) - 1] dr \right] \right\} \tag{107}$$

where $n$ is the number of scatterers per unit volume and $g(r)$ is the radially symmetric pair-distribution function describing the probabilities of the location of neighboring scatterers. This formula is a generalization of the static Maxwell-Garnett formula.

By incorporating the "coherent potential" approach into these approximations, other scattering formulas can be derived [29], with the property that in the low-frequency regime, they simplify to the mixing formula (91).

Also the high-frequency predictions of the Böttcher mixing formula (93) have been studied. Chroud, Pan, Chýlek, and Srivastava have

generalized the effective medium mixing formula to cover the scattering term, naming the effective permittivity formula by DEMA (dynamic effective medium approximation) [51–52]. Application of their theory to the infrared absorption of small palladium-particle composites have proved the validity of the scattering term and the importance of the size distribution of the scatterers in the composite [53].

## 3.5 Numerical Illustrations

In this section, the presented mixing formulas are applied to calculating dielectric properties of geophysical media.

### *a. Tropospheric Attenuation*

First, the microwave attenuation due to rain and hail is studied. Troposphere in the presence of hydrometeors can be treated as a dielectric mixture with air as the host medium and water or ice as inclusions. From the imaginary part of the effective permittivity $\epsilon''_{\text{eff}}$ of this mixture, the absorption attenuation can be calculated:

$$A = \frac{8686\pi}{\lambda}\epsilon''_{\text{eff}} \quad (\text{dB/km}) \tag{108}$$

where the wavelength $\lambda$ has to be given in meters.

It is worth noting that this calculation does not give the scattering loss because the hydrometeors are assumed to be small compared to the wavelength. However, at the frequency of 1 GHz, the ratio of the scattering cross section to the absorption cross section of a raindrop with 1 mm radius is 0.0016 [2]. Hence, at this frequency scattering loss is negligible. The relative permittivity values are, at 1 GHz and the temperature of 0 °C:

$$\epsilon_{\text{air}} = 1 \tag{109}$$

$$\epsilon_{\text{water}} = 87 + i9.7 \tag{110}$$

$$\epsilon_{\text{ice}} = 3.15 + i0.001 \tag{111}$$

To find out the propagation loss of pure rain or pure hail with spherical hydrometeors, the good old Maxwell-Garnett formula is sufficient because the mixture is extremely sparse. With the multilayer sphere mixing formula, the more complicated case of attenuation due

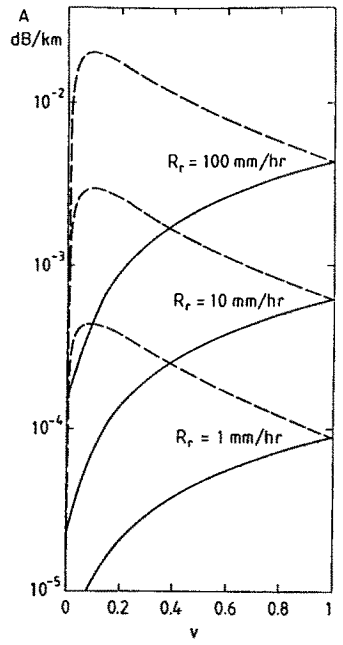


**Figure 3.5 Attenuation of melting hail at 1 GHz (dashed lines) at three different rain rates as a function of the melt volume $v$. The solid line shows the attenuation for the same amount of hydrometeors but in that case hail and rain drops are in the form of separate particles.**

to melting hail can be calculated. In using this, the core of an inclusion is ice and the shell is water. The volume fraction of the hydrometeors $f$ depends on the rain rate [2] (assuming the Marshall-Palmer raindrop distribution, see, for example [54])

$$f = 8.894 \cdot 10^{-8} R_r^{0.84} \frac{1 - 0.083v}{0.917} \tag{112}$$

where $v$ is the ratio of the liquid water volume to the total volume of the hydrometeor and the rain rate $R_r$ has to be given in mm/hr. $v = 0$ corresponds to pure hail and $v = 1$ means pure rain. The number 0.917 in the formula comes from the densities of ice and water: as hail melts ($v$ increases), the hydrometeors shrink and the volume fraction decreases.

The attenuation for three rain rates is shown in Fig. 3.5 as a function of the melt volume $v$. Figure 3.6 shows the attenuation in the case of freezing rain, i.e. the core is water and the shell is ice. This figure

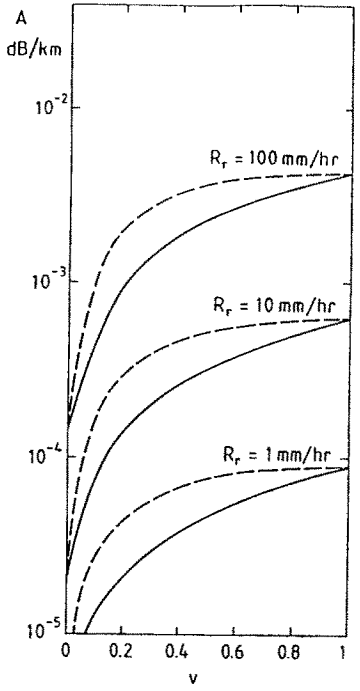


**Figure 3.6 Attenuation of freezing rain at 1 GHz (dashed lines) at three different rain rates as a function of the melt volume $v$. The solid line has the same meaning as in Fig. 3.5.**

is only for theoretical comparison: this kind of hydrometeors probably do not exist in nature. Also shown in both figures is the case where there is the same amount of ice and water in air as in the inhomogeneous two-layer case, but the ice and water droplets form separate homogeneous spheres.

As expected, from the figures it can be seen that the attenuation of rain is much higher than that of the same amount of hail. The figures also show that both inhomogeneous scatterer types (melting hail and freezing rain) attenuate more than in the form of separate scatterers. And what is worth noting is that for melting hail, the attenuation has a strong maximum at the point where where the melt volume is about 0.09, and this value seems to be fairly independent of the rain rate. This means that when hail falls through a warm layer and provided that it melts uniformly from every side, it will be more lossy when partly melted than in the form of water. This effect resembles the "bright band" in radar meteorology: an increased radar backscattering from melting hail, although the physical mechanism is different in these

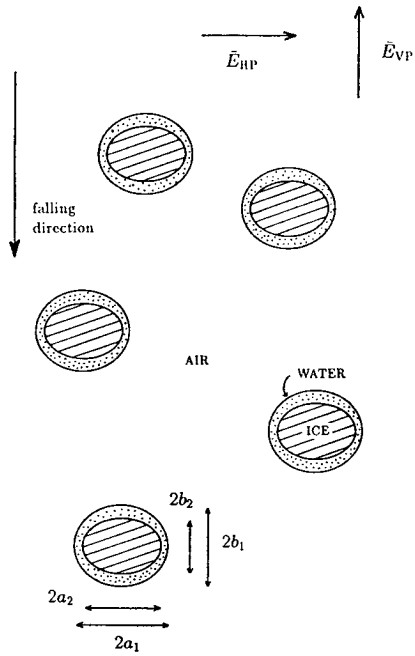


**Figure 3.7 Melting hail modeled as confocal two-layer oblate spheroids that are falling with minor axis vertical.**

two cases: absorption and scattering. However, Hansman has found experimentally also the peaked behavior in the microwave absorption attenuation of melting ice spheres [55]. For more discussion on the subject, see [2].

It is known that falling raindrops are not perfectly spherical but rather oblate spheroids falling with minor axis vertical [56]. The ellipticity of the hydrometeors depends on their size and terminal falling speed. This gives rise to a more sophisticated model for melting hail: a mixture of two-layer confocal oblate ellipsoids of revolution in air according to Fig. 3.7. The attenuation can be calculated using the mixing formulas derived for multilayer ellipsoids. From the confocality requirement, rain rate, and the melt volume, the parameters needed in the formula for the effective permittivity can be calculated (see [5]).

In this case, the attenuation is different for vertically and horizontally polarized waves because the mixture is ordered and therefore anisotropic. The results are shown in Figs. 3.8 and 3.9 at 1 GHz and the rain rate of 100 mm/hr as functions of the melt volume $v$. The

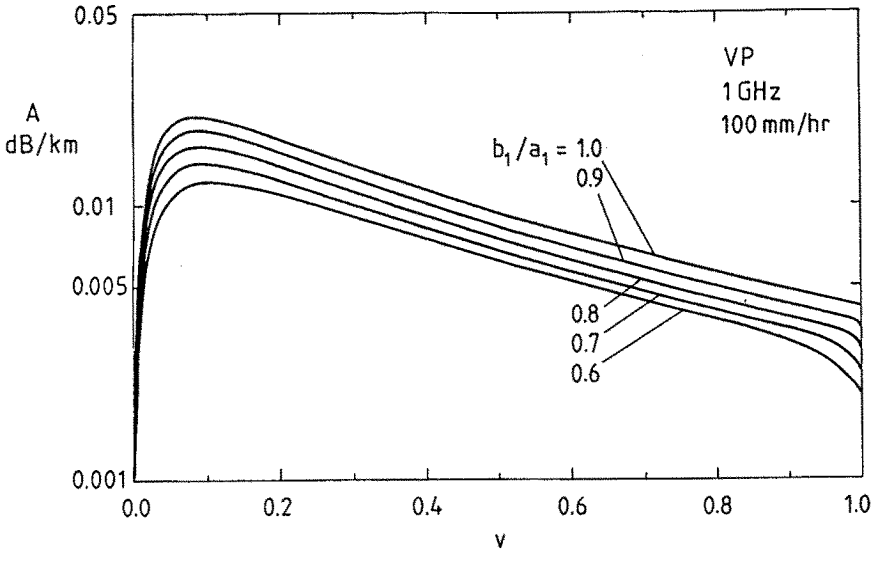


**Figure 3.8 The attenuation of a vertically polarized wave due to melting hail at the frequency of 1 GHz and with the rain rate 100 mm/hr with the axial ratio of the hydrometeor as parameter. The parameter $v$ is the ratio of the liquid water volume to the total volume of the hydrometeor.**

axial ratio of the hydrometeor is a parameter.

The results show that for the spherical case, both horizontally and vertically polarized attenuations are the same, as they should be, and the attenuation curve is the same as in Fig. 3.5. As the hydrometeor begins to deviate from the spherical shape, the horizontally polarized wave will become more attenuated than the vertically polarized wave. This is a result to be expected. The polarization difference is the same as for scattering: increased scattering of the horizontally polarized wave over the vertically polarized wave due to rain is experimentally observed.

There are some limitations in this multilayer ellipsoid model. First, all the hydrometeors are assumed to have the same ellipticity, which is not true at least for rain, where a distribution of different drop sizes is observed. Secondly, the conditions in nature probably do not allow perfect aligning of all hydrometeors. However, the orientation distribution can also be taken care of by following the analysis in [1].

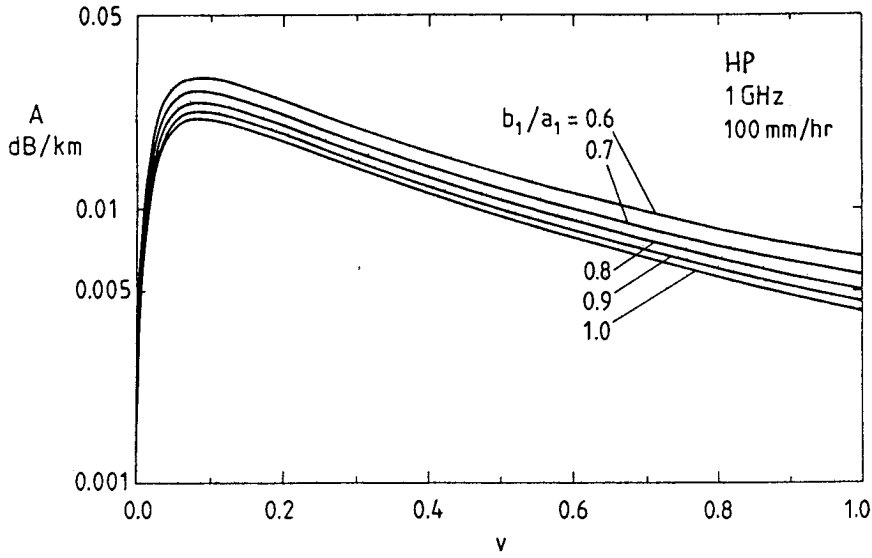


**Figure 3.9 The attenuation of a horizontally polarized wave due to melting hail at the frequency of 1 GHz and with the rain rate 100 mm/hr with the axial ratio of the hydrometeor as parameter. The parameter $v$ is the ratio of the liquid water volume to the total volume of the hydrometeor.**

The third disputable point in the model is the assumption that the melting proceeds in a way that the confocality is preserved.

*b. Snow*

The other application of the presented mixing rules is dry snow modeled as a two-component mixture of air as the background medium and ice inclusions. Ice is practically dispersionless and lossless (relative permittivity about 3.15) in the microwave region which facilitates the theoretical modeling (see reference [57]). Also, experimental data are available on dielectric properties of snow.

The density of snow $\rho_s$ can be calculated from the volume fraction of the ice phase $f_1$ in the following way:

$$\rho_s\,[\mathrm{g/cm^3}] = 0.917 f_1 \tag{113}$$

because the density of ice is 0.917 $\mathrm{g/cm^3}$.

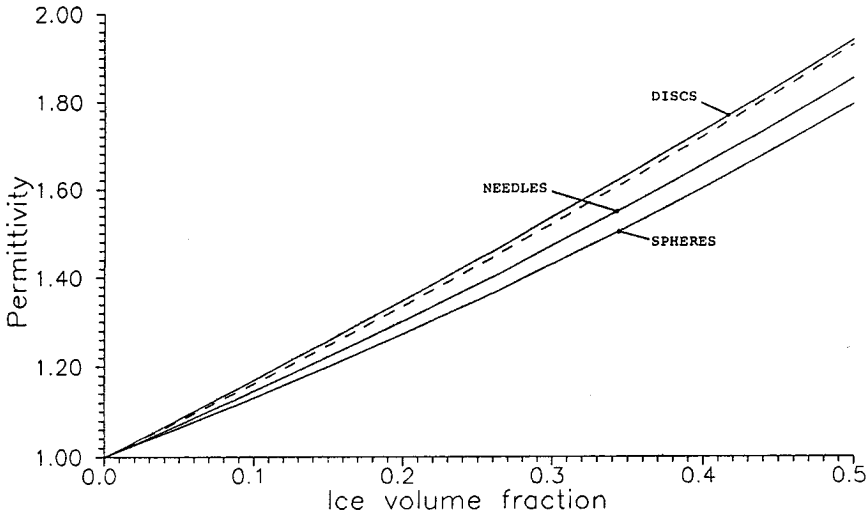


**Figure 3.10 The effective permittivity of dry snow as a function of the ice volume fraction according to Maxwell-Garnett type mixing formulae with spherical, disc-shaped, and needle-shaped ice inclusions. The dashed line is experimental [58]. The accuracy of the experimental curve is $\pm 0.05$.**

First, consider the ice inclusions as homogeneous spheres, discs, or needles that are randomly oriented. The snow permittivity is given by the Maxwell-Garnett-type formulas (24) and (27). Figure 3.10 depicts the results as a function on the ice volume fraction. In the figure, experimental results also are shown according to the model given in [58]:

$$\epsilon_{\text{eff}} = 1 + 1.7\rho_s + 0.7\rho_s^2 \tag{114}$$

where the density has to be given in $\text{g/cm}^3$.

The model of homogeneous ellipsoidal ice scatterers forming snow can easily be criticized by refering to photographs of the microstructure of the snow matrix. Therefore, an alternative model can be applied next: a spherically layered structure of ice and air. At least "depth hoar" type of snow, which is the endproduct of temperature-gradient metamorphism, could be expected to be suitable for this model because

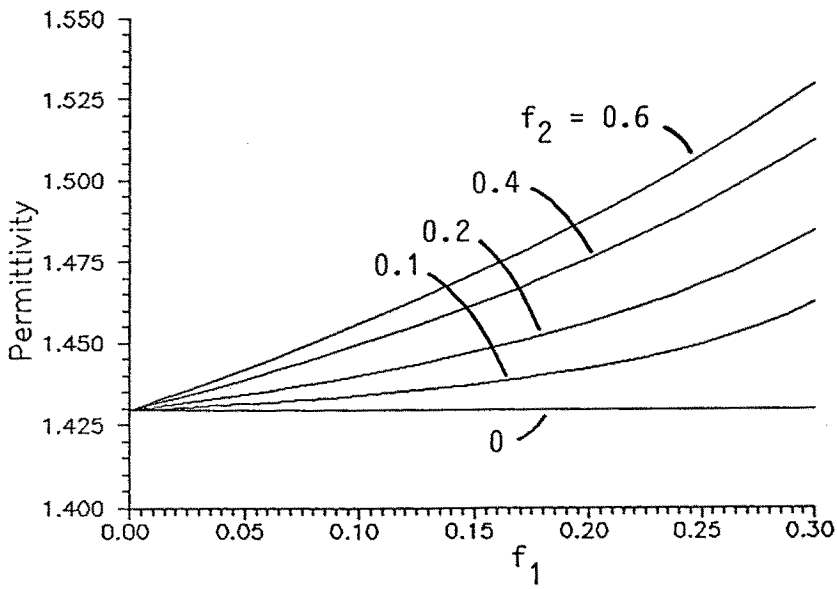


**Figure 3.11 The effective permittivity of dry snow modeled as three-layer ice scatterers in air as a function of the outer layer size and with the size of the hollow space as a parameter. The total fractional volume of ice is 0.3.**

it is observed to form layered ice shells [59].

Consider three-layer ice inclusions where the outermost layer and the core are of ice while the middle layer is air: equation (33) with $N = 3$ and $\epsilon_0 = \epsilon_2 = 1$, and $\epsilon_1 = \epsilon_3 = 3.15$. Figure 3.11 shows the effective permittivity of snow with the total ice volume fraction of 0.3 ($= f_1 + f_3$) as a function of the layer structure parameters. This corresponds to a snow density of 0.28 g/cm$^3$. The core size is the variable and the size of the middle layer is a parameter.

Both figures show that the if the ice phase is assumed to be homogeneous spheres in air, the result is the smallest effective permittivity value for snow, which is, naturally, the Maxwell-Garnett value 1.430. Every deviation of the inclusions from the homogeneous spherical form to the ellipsoidal or layered direction, tends to increase the effective permittivity. In Figure 3.10, all ellipsoidal forms other than the three extreme cases fall between the curves of spheres and discs. Hence, the spherical geometry seems to be a stationary minimum for the effective

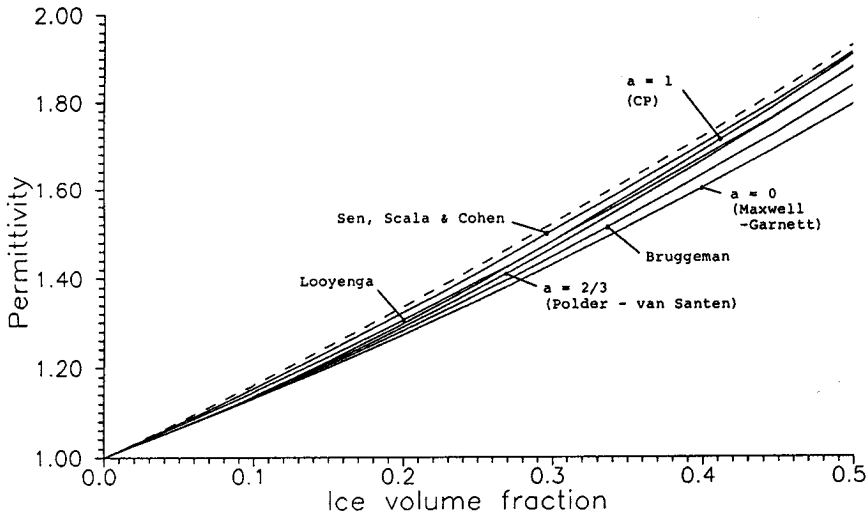


**Figure 3.12 The effective permittivity of dry snow as a function of the ice volume fraction: comparison of different mixing models and experimental values [58] (dashed curve). The accuracy of the experimental curve is $\pm 0.05$.**

permittivity. Snow grains in nature are not spherical. Accurate modeling of snow inevitably calls for more complex geometries, because also the experimental values for the dielectric constant of dry snow $\epsilon_d$ with this density are larger: $\epsilon_d = 1.52$ [58], $\epsilon_d = 1.49$ [27], and $\epsilon_d = 1.62$ [60] . Figure 3.10 also shows this: the accuracy of the experimental curve is $\pm 0.05$, and the spherical geometry predicts results that fall outside the experimental error limit.

Finally, the effect of the choice of apparent permittivity is studied. Different mixing rules follow from the way of taking into account the effect of neighboring inclusions in a mixture. The effective permittivity of dry snow is calculated as a function of its density with mixing formulae of different apparent permittivities, and compared with the experimental curve of equation (114) from reference [58].

The results are shown in graphical form on Fig. 3.12. The observation that the Maxwell-Garnett formula gives the smallest prediction for the effective permittivity of all mixing formulas is here again confirmed. The figure shows also that the predictions of the different models are

close to each other. This is due to the small permittivity contrast between the air and ice phases. Again, looking at the error limits in the experimental curve, $\pm 0.05$, shows that at least the Maxwell-Garnett and Bruggeman models predict too low values for the effective permittivity of dry snow.

## 3.6 Conclusion

In this article, the focus was on polarizabilities, dielectric mixtures, and dielectric modeling questions which are encountered in remote sensing systems monitoring natural media and man-made objects, propagation studies, or even materials science problems excited by the needs of stealth technology. In order to approach the solution, it is necessary to condense the formidable number of degrees of freedom of an electromagnetic problem in a stochastic environment. This can be done by using simpler concepts that still contain most of the relevant structural information of the object. One of these kind of concepts is the use of effective permittivity, which describes macroscopically the dielectric behavior of an inhomogeneous material. Although capable of displaying losses and anisotropy, the effective permittivity, being at the most a complex tensor, disregards the dielectric boundaries on a small scale. The cutoff dimension in applying this permittivity concept is the wavelength of the incident electromagnetic radiation. If the correlation length of the spatial permittivity function of the material is larger than the wavelength, scattering phenomena are no longer negligible and the effective permittivity loses its meaning.

For geophysical media, experimental equations are often used to calculate the macroscopic permittivity from the fractional composition of the material. The mixing rules in this presentation are more sophisticated than those, owing to the fact that these take the internal structure of the mixtures into account. Despite the limited number of geometries, the spherical and ellipsoidal ones, that were under consideration, choices for the microstructure were numerous, as was evident from the dry snow modeling application: homogeneous, layered, and continuously inhomogeneous spheres and ellipsoids. Be there more complex structures, the variational method for solving the effective permittivity is always available. Using the variational approach, no exact analysis but, rather, physical intuition and good guesses are needed, and the method still leads to reasonably accurate results for

this stochastic problem having the discouraging property of possessing no exact solution.

## References

[1] Sihvola, A., and J. A. Kong, "Effective permittivity of dielectric mixtures," *IEEE Trans. on Geosci. Remote Sensing,* **26(4)**, 420–429, July 1988. See also, Corrections, **27(1)**, 101–102, January 1989.

[2] Sihvola, A., "Macroscopic permittivity of dielectric mixtures with application to microwave attenuation of rain and hail," *IEE Proceedings, Part H,* **136(1)**, 24–28, February 1989.

[3] Sihvola, A., and I. V. Lindell, "Transmission line analogy for calculating the effective permittivity of mixtures with multilayer scatterers," *J. of Electromagnetic Waves Applic.,* **2(8)**, 741–756, 1988.

[4] Sihvola, A., and I. V. Lindell, "Polarizability and effective permittivity of layered and continuously inhomogeneous dielectric spheres," *J. of Electromagnetic Waves Applic.,* **3(1)**, 37–60, 1989.

[5] Sihvola, A., and I. V. Lindell "Polarizability and effective permittivity of layered and continuously inhomogeneous dielectric ellipsoids," *J. of Electromagnetic Waves Applic.,* **4(1)**, 1–26, 1990.

[6] Sihvola, A. "Self-consistency aspects of dielectric mixing theories," *IEEE Trans. Geosci. Remote Sensing,* **27(4)**, 403–415, 1989.

[7] Yaghjian, A. D., "Electric dyadic Green's functions in the source region", *Proceedings of the IEEE,* **68(2)**, 248–263, 1980.

[8] Yaghjian, A. D., "Maxwellian and cavity electromagnetic fields within continuous sources," *American J. of Physics,* **53(9)**, 859–863, 1985.

[9] Born, M., and E. Wolf, *Principles of Optics,* Section 2.3.3, Sixth Edition, Pergamon Press, Oxford, 1980.

[10] Robert. P., *Electrical and Magnetic Properties of Materials,* Section 4.3, Artech House, Norwood, Massachusetts, 1988.

[11] Onsager, L., "Electric moments of molecules in liquids," *Journal of the American Chemical Society,* **58(8)**, 1486–1493, August 1936.

[12] Hasted, J. B., *Aqueous Dielectrics,* Section 1.3, Chapman and Hall, London, 1973.

[13] Landau, L. D., and E. M. Lifshitz, *Electrodynamics of Continuous Media,* Sections 4 and 9, Second Edition, Pergamon Press, 1984.

[14] Osborn, J. A., "Demagnetizing factors of the general ellipsoid," *The Physical Review,* **67**, 11–12, 351–357, 1945.

[15] Stoner, E. C., "The demagnetizing factors for ellipsoids," *Philosophical Magazine,* Ser. 7, **36**, 263, 803–821, 1945.

[16] Jackson, J. D., *Classical Electrodynamics,* Second Edition, Chapter 4, John Wiley & Sons, 1975.

[17] Maxwell-Garnett, J. C., "Colours in metal glasses and in metal films," *Transactions of the Royal Society,* **CCIII**, 385–420, London, 1904.

[18] Bohren, C. F., and L. J. Battan, "Radar backscattering of microwaves by spongy ice spheres," *J. of the Atmospheric Sciences,* **39**, 2623–2628, 1982.

[19] Wiener, O., "Zur Theorie der Refraktionskonstanten," *Berichte über die Verhandlungen der königlich sächsischen Gesellschaft der Wissenschaften zu Leipzig,* Math.-Phys. Klasse, **Band 62**, 256–277, Leipzig, 1910.

[20] Pearce, C. A. R., "The electrical conductivity and permittivity of mixtures, with special reference to emulsions of water in fuel oil," *British Journal of Applied Physics,* **6(4)**, 113–120, 1955.

[21] Pearce, C. A. R., "The permittivity of two phase mixtures," *British Journal of Applied Physics,* **6(10)**, 358–360, 1955.

[22] Kong, J. A., *Electromagnetic Wave Theory,* Chapter III, John Wiley & Sons, New York, 1986.

[23] Kellogg, O. D., *Foundations of Potential Theory,* Chapter VII, Dover Publications, New York, 1953.

[24] Bender, C. M., and S. A. Orszag, *Advanced Mathematical Methods for Scientists and Engineers,* McGraw-Hill, 1978.

[25] Harrington, R. F., *Time-harmonic Electromagnetic Fields,*

McGraw-Hill, New York, 1961.

[26] Collin, R. E., *Field Theory of Guided Waves*, McGraw-Hill, New York, 1960.

[27] Mätzler, Ch., "Applications of the interaction of microwaves with the natural snow cover," *Remote Sensing Reviews*, **2**, 259–387, 1987.

[28] Kohler, W. E., and G. C. Papanicolaou, "Some applications of the coherent potential approximation, in *Multiple Scattering and Waves in Random Media*, edited by P. L. Chow, W. E. Kohler, and G. C. Papanicolaou, 199–223, North-Holland Publishing Company, New York, 1981.

[29] Tsang, L., J. A. Kong, and R. T. Shin: *Theory of Microwave Remote Sensing*, Chapters 5.4 and 6.4, Wiley-Interscience, New York, 1985.

[30] Polder, D., and J. H. van Santen, "The effective permeability of mixtures of solids," *Physica*, **XII**, 5, 257–271, 1946.

[31] Taylor, L., "Dielectric properties of mixtures," *IEEE Trans. Ant. Propagation*, **AP-13(6)**, 943–947, 1965.

[32] de Loor, G. P., "Dielectric properties of heterogeneous mixtures," Thesis, Leiden (1956). See also, "Dielectric properties of heterogeneous mixtures with a polar constituent", *Appl. Sci. Res. B*, **11**, 310–320, 1964.

[33] de Loor, G. P., "Dielectric properties of heterogeneous mixtures containing water," *J. of Microwave Power*, **3**, 67–73, 1968.

[34] Böttcher, C. J. F., *Theory of Electric Polarization*, Elsevier, Amsterdam, 1952.

[35] Ambach, W., and A. Denoth, "The dielectric behavior of snow: a study versus liquid water content," *Microwave Remote Sensing of Snowpack Properties*, A. Rango, ed., in *Proc. NASA Workshop*, Fort Collins, Colorado, May 20-22, 1980, NASA Conf. Publ. 2153, 69–92, Washington, DC.

[36] Dobson, M. C., F. T. Ulaby, M. T. Hallikainen, and M. A. El-Rayes "Microwave dielectric behavior of wet soil — Part II: Dielectric mixing models," *IEEE Trans. Geosci. Remote Sensing*, **23(2)**, 35–46, 1985.

[37] Sihvola, A., E. Nyfors, and M. Tiuri, "Mixing formulae and experimental results for the dielectric constant of snow," *J. of Glaciology,* **31**, 108, 163–170, 1985.

[38] Looyenga, H., "Dielectric constants of mixtures," *Physica,* **31**, 401–406, 1965.

[39] Bruggeman, D. A. G., "Berechnung verschiedener physikalischer Konstanten von heterogenen Substanzen, I. Dielektrizitätskonstanten und Leitfähigkeiten der Mischkörper aus isotropen Substanzen," *Annalen der Physik,* 5. Folge, **Band 24**, 636–664, 1935.

[40] Sen, P. N., C. Scala, and M. H. Cohen, "A self-similar model for sedimentary rocks with application to the dielectric constant of fused glass beads," *Geophysics,* **46(5)**, 781–795, 1981.

[41] Birchak, J. R., L. G. Gardner, J. W. Hipp, and J. M. Victor, "High dielectric constant microwave probes for sensing soil moisture," *Proceedings of the IEEE,* **62(1)**, 93–98, 1974.

[42] Lichtenecker, K., "Mischkörpertheorie als Wahrscheinlichkeitsproblem," *Physikalische Zeitschrift,* 30. Jahrgang, **Nr. 22**, 805–809, 1929.

[43] Lichtenecker, K., and K. Rother, "Die Herleitung des logarithmischen Mischungsgesetzes als allgemeinen Prinzipien der stationären Strömung," *Physikalische Zeitschrift,,* 32. Jahrgang, **Nr. 6**, 255–260, 1931.

[44] Abramowitz, M., and I. A. Stegun (eds.), *Handbook of Mathematical Functions with Formulas, Graphs, and Mathematical Tables,* Formula 4.2.21, Dover, New York, 1972.

[45] Runge, I., "Zur elektrischer Leitfähigkeit metallischer Aggregate," *Zeitschrift für technische Physik,* 6. Jahrgang, **Nr. 2**, 61–68, 1925.

[46] Meredith, R. E., and C. W. Tobias, "Resistance to potential flow through a cubical array of spheres, *J. Applied Physics,* **31(7)**, 1270–1273, 1960.

[47] Tinga, W. R., W. A. G. Voss, and D. F. Blossey, "Generalized approach to multiphase dielectric mixture theory," *J. Applied Physics,* **44(9)**, 3897–3902, 1973.

[48] Wait, J. R., *Electromagnetic Wave Theory,* Section 2.3, Harper & Row, New York, 1985.

[49] Bohren, C. F., and D. R. Huffman, *Absorption and Scattering of Light by Small Particles,* Section 5.4, John Wiley & Sons, 1983.

[50] Poularikas, A. D., "Effective index of refraction of isotropic media containing layered spheres," *J. Applied Physics,* **58(2)**, 1044–1046, 1985.

[51] Stroud, D., and F. P. Pan, "Self-consistent approach to electromagnetic wave propagation in composite media: Application to model granular metals," *Physical Review B,* **17(4)**, 1602–1610, 1978.

[52] Chýlek, P., and V. Srivastava, "Dielectric constant of a composite inhomogeneous medium," *Physical Review B,* **27(8)**, 5098–5106, 1983.

[53] Chýlek, P., D. Boise, and R. G. Pinnick, "Far-infrared absorption of small palladium-particle composites," *Physical Review B,* **27(8)**, 5107–5109, 1983.

[54] Ulaby, F. T., R. K. Moore, and A. K. Fung, *Microwave remote sensing: active and passive,* Part I, p. 317, Addison-Wesley Publishing Company, Reading, Massachusetts, 1981.

[55] Hansman, R. J., Jr., "Microwave absorption measurements of melting spherical and nonspherical hydrometeors," *J. Atmos. Sci.,* **43**, 1643–1649, 1986.

[56] Doviak, R. J., and D. S. Zrnić, *Doppler Radar and Weather Observations,* Chapter 8, Academic Press, Orlando, Florida, 1984.

[57] Mätzler, Ch., and U. Wegmüller, "Dielectric properties of freshwater ice at microwave frequencies," *J. Phys. D: Appl. Phys.* (UK), 20, 1623–1630, 1987.

[58] M. E. Tiuri, A. H. Sihvola, E. G. Nyfors, and M. T. Hallikainen, "The complex dielectric constant of snow at microwave frequencies," *IEEE J. Oceanic Engineering,* **9(5)**, 377–382, 1984.

[59] LaChapelle, E. R., *Field Guide to Snow Crystals,* University of Washington Press, Seattle and London, 1969.

[60] Denoth, A., A. Foglar, P. Weiland, C. Mätzler, H. Aebischer, M. Tiuri, and A. Sihvola, "A comparative study of instruments for measuring the liquid water content of snow," *J. Applied Physics,* **56(7)**, 2154–2160, 1984.